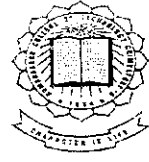




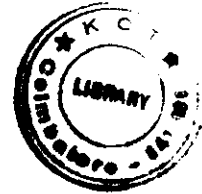
Fuzzy Logic Approach for Broken Rotor Bar and End ring fault Detection in Induction Motor



A Project Report

Submitted by

T. Moorthi - 71203105300
A. Indrakumar - 71203105301
K. Hemarajan - 71203105302
P. V. Vineeth - 71203105306



P-2084

In partial fulfillment for the award of the Degree

of

Bachelor of Engineering

in

Electrical and Electronics Engineering

**DEPARTMENT OF ELECTRICAL AND ELECTRONICS
ENGINEERING**

KUMARAGURU COLLEGE OF TECHNOLOGY

COIMBATORE - 641006

ANNA UNIVERSITY: CHENNAI 600 025

APRIL 2007

ANNA UNIVERSITY: CHENNAI 600 025

BONAFIED CERTIFICATE

Certified that this project report entitled “Fuzzy Logic Approach for Broken Rotor bar and End ring fault Detection in Induction motor” is the bonafied work of

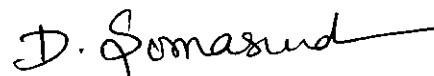
Mr. T. Moorthi	-	Register No. 71203105300
Mr. A. Indrakumar	-	Register No. 71203105301
Mr. K. Hemarajan	-	Register No. 71203105302
Mr. P. V. Vineeth	-	Register No. 71203105306

Who carried out the project work under my supervision.



Signature of the Head of the Department

Prof. K. Regupathy Subramanian



Signature of the Guide

Mrs. D. Somasundareswari

Certified that the candidate with university Register No. was examined in
Project viva voce Examination held on 26-4-07



Internal Examiner

26/4/07



External Examiner

**DEPARTMENT OF ELECTRICAL AND ELECTRONICS ENGINEERING
KUMARAGURU COLLEGE OF TECHNOLOGY, COIMBATORE – 641006**

ABSTRACT

Induction motors are very essential in industrial field. Variety of faults occurs in this machine. Broken rotor bar and end ring fault yields asymmetrical operation of the induction machine causing unbalanced current, torque pulsation, increased losses and decreased average torque. This leads to motor malfunction and causes serious damage to the stator windings if left undetected. To prevent such damage, the fault should be detected at the earliest.

A simple and reliable On-Line technique for broken rotor bar and end ring detection based on stator current spectrum analysis is developed in this project. A Real Time Analyzer is used to monitor the stator current spectrum. The fault signature is extracted from the stator current spectrum. The Fuzzy Logic is used to diagnose the faults.

ACKNOWLEDGEMENT

We are highly privileged to thank our principal **Dr. Joseph V. Thanikal**, M.E., Ph.D., PDF, CEPIT, for supporting us.

We express our grateful thanks to **Prof. K. Regupathy Subramanian**, B.E (Hons), M.Sc., MIEEE, IES, Head of Department, Electrical and Electronics Engineering, Kumaraguru College of Technology, for the facilities made available for the progress and completion of this project.

We are highly indebted to thank our guide **Mrs.D.Somasundareswari**, ME, Senior Lecturer, Department of Electrical and Electronics Engineering, Kumaraguru College of Technology, for her invaluable guidance and continuous encouragement for the successful completion of this project.

Our sincere thanks to **Dr. V. Duraisamy**, M.E., Ph.D., MISTE, AMIE, MIEEE, Professor, Electrical and Electronics Engineering Department, Kumaraguru College of Technology, who have provided valuable suggestions and immense support throughout this project.

We thank the teaching and non-teaching staff of Electrical and Electronics Engineering Department for their support and co-operation.

CONTENTS

Title	Page no.
Bonafied Certificate	ii
Abstract	iii
Acknowledgement	iv
Contents	v
List of Tables	viii
List of Figures / Photos	ix
Symbols, Abbreviations of Nomenclature	xi
CHAPTER 1 INTRODUCTION	1
1.1 Necessity of Fault Detection	2
1.2 Causes for Failure	3
1.3 Objective	4
1.4 Organization of the Report	4
CHAPTER 2 THREE PHASE INDUCTION MOTOR	6
2.1 Introduction	7
2.2 Effect of Rotor Asymmetry	8
2.2.1 Modeling of Healthy Induction Motor	8
2.2.2 Modeling of Broken Rotor Bars	9
2.2.2.1 Rotor Asymmetry due to broken End Ring	10
2.2.3 Modeling of Broken End Rings	11
2.2.3.1 Rotor Asymmetry due to broken Rotor bars	12
2.3 Methodology	13
CHAPTER 3 EXPERIMENTAL SETUP FOR DATA ACQUISITION	15
3.1 Hardware Description	16
3.1.1 Experimental Hardware Setup	16
3.1.2 Component Specification	17
3.1.2.1 Induction motor specification	17
3.1.2.2 Current Transformer	18
3.1.2.3 Rheostat	18
3.1.2.4 Stereo Cable	18

3.1.2.5	A/D Converter	18
3.1.2.6	Real Time Analyzer	18
3.1.2.7	Fuzzy Logic	18
3.1.3	Lower Sideband and Upper sideband Frequency	19
3.2	Software Description	19
3.2.1	Real Time Analyzer	19
3.2.1.1	Oscilloscope	20
3.2.1.2	Recorder	21
3.2.1.3	FFT analyzer	22
3.3	Experimental Results	23
3.3.1	Broken Rotor Bar on No-load condition	24
3.3.1.1	Stator current spectrum at various broken bar conditions	24
3.3.1.2	Harmonic Amplitudes	28
3.3.2	Broken Rotor Bar at half-load condition	29
3.3.2.1	Stator current spectrum at half-load condition	29
3.3.2.2	Harmonic Amplitudes	32
3.3.3	Broken End ring condition	32
3.3.3.1	Stator current spectrum	33
3.3.3.2	Harmonic Amplitudes	35
CHAPTER 4	FUZZY LOGIC BASED FAULT DIAGNOSIS	36
4.1	Introduction	37
4.2	Mamdani Fuzzy Inference System	38
4.2.1	Fuzzifier	39
4.2.2	Knowledge Base	39
4.2.3	Inference Engine	39
4.2.4	Defuzzifier	39
4.2.5	Operation of Fuzzy system	40
4.3	Fault Diagnosis for Broken Rotor Bar	41
4.3.1	Rules	41
4.3.2	Fuzzification	41
4.3.3	Simulation Result	43

4.4	Fault Diagnosis for Broken End ring	44
4.4.1	Rules	45
4.4.2	Fuzzification	45
4.4.3	Simulation Result	46
4.5	Software Design	47
4.5.1	Algorithm	47
4.5.2	Flowchart	48
CHAPTER 5	CONCLUSION	50
5.1	Conclusion of the project	51
5.2	Future Scope	51
	APPENDIX	52
	REFERENCES	57
	BIBLIOGRAPHY	59

LIST OF TABLES

Table	Title	Page No.
3.1	Harmonic Amplitudes for No-load condition in Broken Rotor Bar	28
3.2	Harmonic Amplitudes for Load Condition in Broken Rotor Bar	32
3.3	Harmonic Amplitudes for Broken End Ring	35
4.1	Simulation result of broken rotor bar in no-load condition	43
4.2	Simulation result of broken rotor bar in load condition	44
4.3	Simulation result for broken end ring	46

LIST OF FIGURES

Figure No.	Title	Page No.
1.1	Induction Motor fault Statistics	2
2.1	Rotor construction of an Induction motor	7
2.2	Modeling of Healthy Induction motor	8
2.3	Modeling of Broken rotor bar	9
2.4	Modeling of Broken end ring	11
2.5	Schematic diagram of Methodology	14
3.1	Hardware setup	16
3.2	Photographic view of setup	16
3.3	Real time analyzer	20
3.4	Oscilloscope	21
3.5	Recorder	22
3.6	FFT Analyzer	23
3.7	Photographic view of broken bar	24
3.8	Stator Current Spectrum of healthy motor in no-load condition	24
3.9	Stator Current Spectrum at one Broken rotor Bar in no-load condition	25
3.10	Stator Current Spectrum at two broken rotor bar in no-load condition	25
3.11	Stator Current Spectrum at three Broken rotor bar in no-load condition	26
3.12	Stator Current Spectrum at four broken rotor bar in no-load condition	26
3.13	Stator Current Spectrum at five broken rotor bars in no-load condition	27
3.14	Stator Current Spectrum at six broken rotor bars in no-load condition	27
3.15	Stator Current Spectrum at seven broken rotor bars in no-load condition	27

3.16	Stator Current Spectrum at one broken rotor bar in load condition	29
3.17	Stator Current Spectrum at two broken rotor bars in load condition	29
3.18	Stator Current Spectrum at three broken rotor bars in load condition	30
3.19	Stator Current Spectrum at four broken rotor bars in load condition	30
3.20	Stator Current Spectrum at five broken rotor bars in load condition	30
3.21	Stator Current Spectrum at six broken rotor bars in load condition	31
3.22	Stator Current Spectrum at seven broken rotor bars in load condition	31
3.23	Photographic view of broken end ring	33
3.24	Stator Current Spectrum at one broken section in end ring	33
3.25	Stator Current Spectrum at two broken sections in end ring	34
3.26	Stator Current Spectrum at three broken sections in end ring	34
3.27	Stator Current Spectrum at four broken sections in end ring	34
4.1	Mamdani fuzzy inference System	38
4.2	Fuzzy systems	40
4.3	Membership function for A1	42
4.4	Membership function for A2	42
4.5	Membership function for output	42
4.6	Membership function for input	45
4.7	Membership function for output	46
4.8	Flowchart of Software algorithm	48
4.9	Picture of the Software	49

SYMBOLS AND ABBREVIATIONS

emf	electro motive force
mmf	magneto motive force
i_{rk}	rotor circuit current
i_{re}	circulating current
KVL	Kirchhoff's voltage law
f_1	supply frequency
f_2	slip frequency
f_{sb}	sideband frequency
s	slip
CT	current transformer
CRO	cathode ray oscilloscope
Rpm	revolutions per minute
rms	root mean square
FFT	fast Fourier transform
A/D	analog to digital converter
D/A	digital to analog converter
A1, A2	amplitude at 46Hz, amplitude at 54Hz
FL	fuzzy logic
Ns	synchronous speed
N	rotor speed
dB	decibels
pk-pk	peak to peak

CHAPTER-1
INTRODUCTION

CHAPTER-1 INTRODUCTION

Induction motors are a critical component of many industrial processes and are frequently integrated in commercially available equipment. Safety, reliability, efficiency, and performance are some of the major concerns of induction motor applications. With issues such as aging motors, high reliability requirements, and cost competitiveness, the issues of induction motors fault detection and diagnosis are of increasing importance. Of these Broken rotor bar and end ring fault yields asymmetrical operation of the induction machine causing unbalanced current, torque pulsation, increased losses and decreased average torque. This leads to motor malfunction and causes serious damage to the stator windings if left undetected. Earlier detection of the fault reduces repair cost and motor outage time thereby improving safety.

1.1 NECESSITY OF FAULT DETECTION

Figure 1.1 shows the fault statistics of induction motor. The statistical data of failures among utility size motors indicated that 10% of the induction motor failures were rotor related. Rotor related faults in three phase induction motors are due to broken bars and end rings. The root of the failure is the crack that develops in the rotor bars. The crack may increase its size if left undetected.

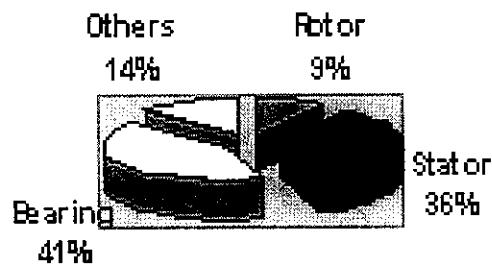


Figure 1.1 Induction Motor fault statistics

Faults involving several broken bars cause excessive vibration, noise and sparking during motor starting. Fabricated type rotors have more incidents of rotor bar breakage than cast rotors. On the other hand, cast rotors are more difficult to repair once they fail. Once a bar breaks, the condition of the neighboring bars also deteriorates progressively due to increased stresses. To prevent such a cumulative destructive process, the problem should be detected early, that is, when the bars are beginning to crack.

Broken bars and end rings can be a serious problem when Induction motors have to perform hard duty cycles. Broken rotors and end rings do not initially cause an Induction motor to fail, but they can impair motor performance, lead to motor malfunction, and cause severe mechanical damage to the stator winding if left undetected. Moreover, an Induction motor with broken bars and end rings cannot operate in dangerous environments due to sparking at the fault site. For these reasons, broken rotors should be taken care of during the initial stage itself and further damage can be prevented.

1.2 CAUSES FOR FAILURE

- The reasons for rotor bar and end ring breakage are several. They can be caused by,
- a) **Thermal stresses** due to thermal overload and unbalance, hot spots or excessive losses, sparking (mainly fabricated rotors),
 - b) **Magnetic stresses** caused by electromagnetic forces, unbalanced magnetic pull, electromagnetic noise and vibration,
 - c) **Residual stresses** due to manufacturing problems,
 - d) **Dynamic stresses** arising from shaft torques, centrifugal forces and cyclic stresses,
 - e) **Environmental stresses** caused by for example contamination and abrasion of rotor material due to chemicals or moisture,
 - f) **Mechanical stresses** due to loose laminations, fatigued parts, bearing failure etc.
 - g) **Other problems** include misapplication, poor design practices, and manufacturing variations.

1.3 OBJECTIVE

- ❖ To detect broken rotor bar and end ring faults in three phase squirrel cage Induction motor
- ❖ To reduce computational complexity

1.4 ORGANISATION OF THE REPORT

Chapter 1, Introduction

Deals with the problems that occur in the induction machines, mainly rotor bar and end ring failures. The various causes of the rotor bar and end ring failure, the necessity of finding them and the effects produced by them are discussed.

Chapter 2, Three phase Induction motor

Deals with the importance of the induction motors, their operating principle and various types of rotor construction. The effects of the broken rotor bar and end ring are discussed in a single line representation.

Chapter 3, Experimental Setup for Data Acquisition

Deals with the sequence of process that is to be carried out to produce the results. The hardware setup for online monitoring, for the detection of broken rotor bar and end ring at both no-load condition and load condition. The various components used in the hardware set up are described with their specification.

Deals with the software “Real Time Analyzer” used for our project to record the stator current spectrum. The main functions of the real time analyzer like oscilloscope, recorder and FFT analyzer are discussed in detail. The current spectrum taken under various faulty conditions are analyzed and the harmonic amplitudes under various conditions are tabulated.

Chapter 4, Fuzzy Logic Based Fault Diagnosis

Gives the importance and advantage of using this fuzzy logic approach. Describes the mamdani system used for doing the Fuzzification. Explains the simulated result and calculates the percentage of error for depicting the performance of this diagnosis.

A Software called broken rotor bar and end ring fault detector is designed to obtain the stator current spectrum, amplitude levels and to check the status of the same.

Chapter 5, Conclusion

The main objective that is set and achieved through this project. The future enhancement that can be produced with this approach.

CHAPTER-2
THREE PHASE INDUCTION MOTOR

CHAPTER-2

THREE PHASE INDUCTION MOTOR

2.1 INTRODUCTION

Three-phase induction machines are asynchronous speed machines, operating below synchronous speed when motoring and above synchronous speed when generating. The cage type electrical motor has electrical circuits on both sides i.e., on stator and rotor but all the external electrical input is fed into the stator circuit only. There are no rubbing contacts needed to make electrical connections from stationary environment to the rotating motor.

When the three-phase stator windings are fed by a three-phase supply then, a magnetic flux of constant magnitude, but rotating at synchronous speed is set up. The flux passes through the air gap, sweeps past through the rotor surface and so cuts the rotor conductors which as yet are stationary. Due to the relative speed between the rotating flux and the stationary conductors, an e.m.f is induced in the latter, according to faraday's law of electro-magnetic induction. Since the rotor bars or conductors form a closed circuit, rotor current is produced whose direction as given by Lenz's law, is such as to oppose the very cause producing it. In this case, the cause which produces the rotor current is the relative velocity between the rotating flux of the stator and the stationary rotor conductors. Hence, to reduce the relative speed, the rotor starts running in the same direction as that of the flux and tries to catch up with the rotating flux.

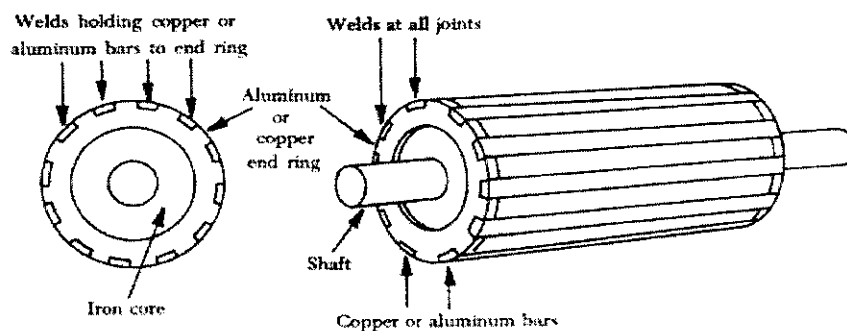


Figure 2.1 Rotor construction of an Induction motor

Almost 90 percent of induction motors are squirrel-cage type, because this type of rotor has the simplest and most rugged construction and is almost indestructible. The rotor as in Figure 2.1, consist of a cylindrical laminated core with parallel slots for carrying the rotor conductors, which are not wire but consists of heavy bars of copper, aluminum or alloys. One bar is placed in each slot rather the bars are inserted from the end when semi-closed slots are used. The rotor bars are brazed or electrically welded or bolted to two heavy and stout short-circuiting end-rings.

The rotor bars are permanently short-circuited on themselves; hence it is not possible to add any external resistance in series with the rotor circuit for starting purposes.

2.2 EFFECT OF ROTOR ASYMMETRY

The flow of current in the Rotor circuit can be represented by a single line diagram. This representation is used to describe the modeling of Broken Rotor bar and End Ring. The current flow affected by these conditions can be easier to understand with the help of these diagrams.

2.2.1 Modeling of Healthy Induction Motor

The Figure 2.2 shows the current flow representation of a healthy induction motor. In this single line representation there is no broken rotor bars or broken end rings.

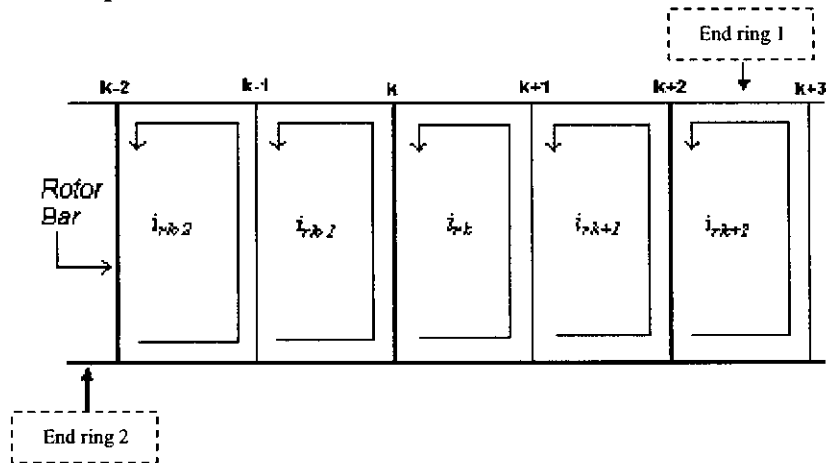


Figure 2.2 Modeling of Healthy Induction motor

The horizontal lines represent the End rings and the vertical lines represent the rotor bars. Two rotor bars and its connector are represented as a single circuit. And separate

currents flow in each circuit and all are equal loops. The rotor current loop is represented as i_{rk} and the representation changes at different bars. The i_{rk} is the Rotor circuit current.

2.2.2 Modeling of Broken Rotor Bars:

The Figure 2.3 shows the current flow representation of a Broken Rotor circuit and a healthy End ring (connector). As a result there will be uneven current flow in the rotor-connector circuit where the Broken Rotor Bar is present with respect to other circuits. There are different approaches to the modeling of Broken Rotor Bar.

One approach is to represent the broken bar with a very high resistance leaving the circuit topology unchanged.

And the second approach is to modify the circuit topology by removing the broken bar from the circuit KVL formation.

Here the second approach has been adopted because, (1) the implementation of a broken bar by a very high resistance could introduce numerical ill-conditioning and instability, and (2) each time a broken bar is removed, it reduces the simulation time.

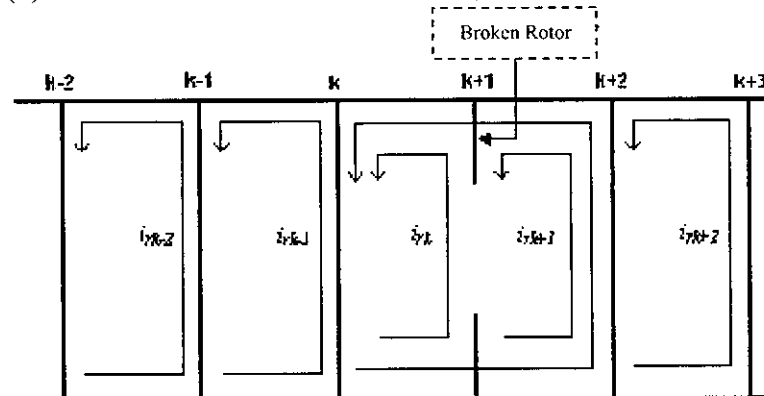


Figure 2.3 Modeling of Broken rotor bar

In the diagram vertical line shows the Rotor bar, where the $(k+1)$ th Bar is broken. The figure shows the five adjacent rotor circuits with current labeled, i_{rk-2} , i_{rk-1} , i_{rk} , i_{rk+1} , i_{rk+2} , respectively in which $(k+1)$ th bar is broken. Due to the $(k+1)$ th broken bar, the rotor circuit currents, i_{rk} and i_{rk+1} , are required to be equal and this current is now forced to flow in the double-width rotor circuit comprising the k th and $(k+1)$ th rotor loops as shown in the figure. Broken rotor at different places may lead to more double width rotor current which affects the stator current in turn. So if the number of broken bars is getting increased, these leads to more harmonics in the stator current.

So, proper monitoring must be done to identify the presence of these harmonics. By close examination of the flux plot in an asymmetrical (with broken bars), it can be noticed that the region around the broken bar of the rotor has a high degree of magnetic saturation in comparison to the same region of flux plot in a symmetrical (with no broken bars). This is due to the fact that in the broken bar region there is no localized rotor conductor demagnetization effect since these bars carry no slip-frequency currents. This heavy localized magnetic saturation has an irregularity effect on the motor's winding inductance profiles, and an inevitable effect on the stator and rotor core loss distributions. That is, such an event can create a non-uniform distribution of core loss, particularly in the rotor and can result in localized hot spots in the rotor. Such hot spots can lead to excessive heating in the adjacent bars, and thus with time and depending on the duty cycle of the motor, these adjacent bars can become more susceptible to wear, thermal stress and eventual breaking.

2.2.2.1 Rotor asymmetry due to broken Rotor bars

In case of an Induction motor the 3-phase symmetrical stator winding fed from a symmetrical supply with frequency f_1 , will produce a resultant forward rotating magnetic field at synchronous speed and if exact symmetry exists there will be no resultant backward rotating field. Any asymmetry of the supply or stator winding impedances will cause a resultant backward rotating field from the stator winding. When applying the same rotating magnetic field fundamentals to the rotor winding, the first difference compared to the stator winding is that the frequency of the induced electro-magnetic force and current in the rotor winding is at slip frequency, *i.e.* $s*f_1$ and not at the supply frequency.

The rotor currents in a cage winding produce an effective 3-phase magnetic field with the same number of poles as the stator field but rotating at slip frequency, $f_2 = s*f_1$ with respect to the rotating rotor. With a symmetrical cage winding, only a forward rotating field exists. If rotor asymmetry occurs then there will also be a resultant backward rotating field at slip frequency with respect to the forward rotating rotor. As a result, the backward rotating field with respect to the rotor induces an e.m.f. and current in the stator winding at:

$$f_{sb} = f(1-2s) \text{ Hz} \quad \text{-----} \rightarrow \quad (1)$$

The Equation.1 is referred to as the lower twice slip frequency sideband due to broken rotor bars. Therefore a cyclic variation of current that causes a torque pulsation at

twice slip frequency ($2sf_1$) and a corresponding speed oscillation, which is also a function of the drive inertia.

This speed oscillation can reduce the magnitude (amps) of the $f_1(1-2s)$ sidebands but an upper sideband current component at $f_1(1+2s)$ is induced in the stator winding due to rotor oscillation. The upper sideband is enhanced by the third time harmonic flux. Broken rotor bars therefore result in current components being induced in the stator winding at frequencies given by

$$f_{sb} = f_1(1 \pm 2s) \text{ Hz} \quad \text{-----> (2)}$$

The Equation.2 is the classical twice slip frequency sidebands due to broken rotor bars. These two frequency components show predominant variation in their amplitudes and these two components are taken for the analysis under various broken bar and end ring conditions.

2.2.3 Modeling of Broken End Rings:

The modeling approach adopted here is similar to that adopted in the broken bar case. That is, broken rotor end-ring connector segments are not modeled by representing the broken segments by very high resistance. A broken end-ring connector segment is modeled by a non-zero circulating current, i_{re} , in the connector as shown in the figure.

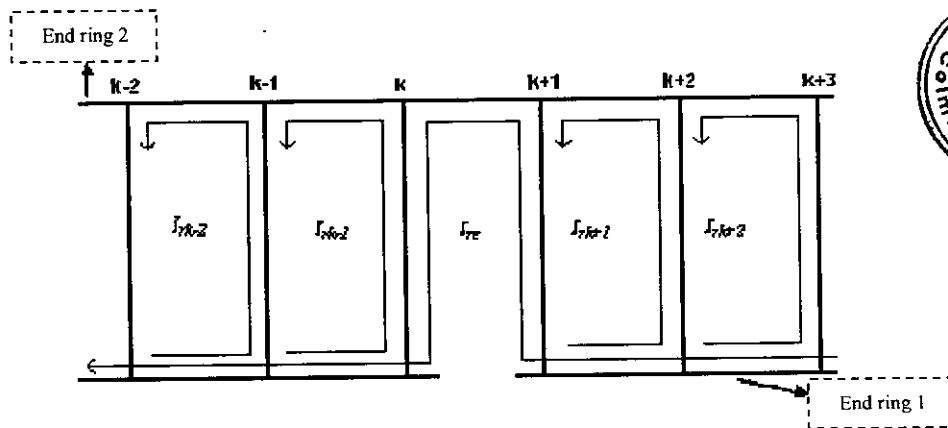


Figure 2.4 Modeling of Broken end ring

The Figure 2.4 shows the representation of current flow in broken end ring. The horizontal line shows the two end rings with a broken section between the rotor bar k and $(k+1)$. It should be noted that no matter where the broken end-ring connector segments are located along the circumference of the rotor, the fault condition is still represented by a single

non-zero circulating current, i_{re} , which flows in all the bars separated by their respective broken connector segments.

These broken connector segments can be got due to high thermal stress or mechanical stress, etc. Broken sections at various connector segments may lead to high value of circulating current, which in turn has effect on those stator currents. So, the monitoring of this stator current is necessary to identify the fault in the end-ring connectors.

By observing the magnetic field pattern as in the case of broken bars, it is not symmetrical. The region in the vicinity of the broken connectors has a high degree of magnetic saturation that has distortive effect on winding inductance profiles as explained in the broken bar segment.

2.2.3.1 Rotor asymmetry due to broken end ring

Under normal operating conditions, an R Y B positive sequence of 3-phase balanced input terminal voltages impressed upon the 3-phase R Y B of the stator armature produces a non-zero forward rotating field in the air gap of induction motor. This forward rotating field in the air gap of the motor consequently induces slip frequency currents in the rotor bars and end ring respectively. This induced rotor currents then produce forward and backward rotating field in the air gap of the motor.

For a symmetrical rotor the resultant of backward rotating field is zero, while the resultant of forward rotating field is non-zero. However under any abnormal condition that destroys the symmetry of the rotor, the backward rotating field is no longer zero.

It is the ultimate identification of the effects of this non-zero resultant backward rotating field that forms the basis for the on-line monitoring technique. In other words when a rotor bar is assumed to be insulated from the rotor core is broken, and then no current flows in the bar. The resulting asymmetry in the rotor results in a non-zero backward rotating field that rotates at slip frequency speed with respect to the rotor. This non-zero rotating field induces harmonic currents in the stator windings, which are superimposed on the stator winding currents at a frequency of

$$(1-2s) f_1 \quad \text{-----} \rightarrow \quad (3)$$

Where s is the operating slip and f_1 is the fundamental (stator) supply frequency. This induced current in the stator-winding manifest themselves as a sideband, $(-2sf_1)$, near the fundamental frequency of the power supply.

2.3 METHODOLOGY

The figure 2.5 shows the schematic diagram of methodology. The stator current spectrum is converted into an equivalent voltage and recorded by giving it as the input to the microphone input terminal of the PC by means of a stereo cable. The current waveform can be recorded by, Online monitoring, where motor is always connected to supply.

The input voltage level to the PC sound card is being adjusted by means of a rheostat to the acceptable level of the sound card. It is normally 1v pk-pk. The current spectrums are recorded for various numbers of broken rotors and end ring.

Fast Fourier transform is done on the recorded waveforms by means of the FFT analyzer. The output of the FFT analyzer will be in one of the following forms: spectrum, octave band or waterfall model. It will be an amplitude Vs frequency graph. The amplitude of the various frequency components are thus displayed in dB. The values can also be recorded by means of using the option data recorder provided by the FFT analyzer. The amplitudes of the two side band components at frequencies $(1+2s)f$ and $(1-2s)f$ are being noted down and the values are tabulated for various broken bar conditions.

The diagnosis of the faults is done by means of fuzzy logic. Fuzzy logic based systems have been successfully implemented to classify broken rotor bar and end ring faults by categorizing the $(1\pm 2s)f$ components by a set of rules. Each of these sideband components is described by membership functions like 'small', 'medium' and 'large'. The fuzzy logic system considered is the mamdani type. The fuzzy inference is performed by using the various fuzzy implication methods and the results are being compared in each case. A typical rule might read like "If lower side band is larger and the upper sideband is medium then there is one or two broken bars."

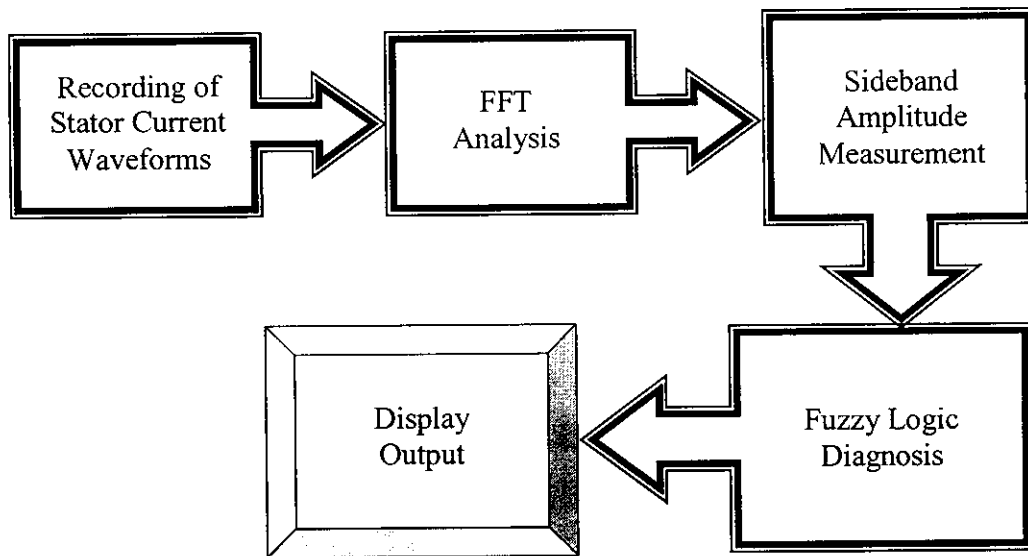


Figure 2.5 Schematic diagram of Methodology

CHAPTER-3
EXPERIMENTAL SETUP FOR DATA ACQUISITION

CHAPTER-3
EXPERIMENTAL SETUP FOR DATA ACQUISITION

3.1 HARDWARE DESCRIPTION

3.1.1 Experimental Hardware Setup

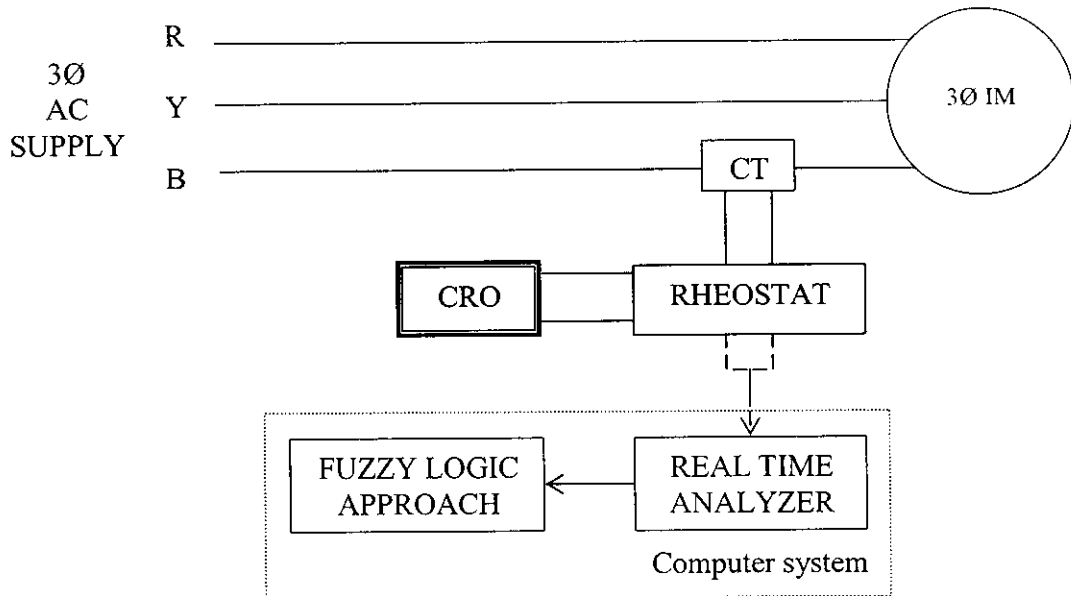


Figure 3.1 Hardware setup

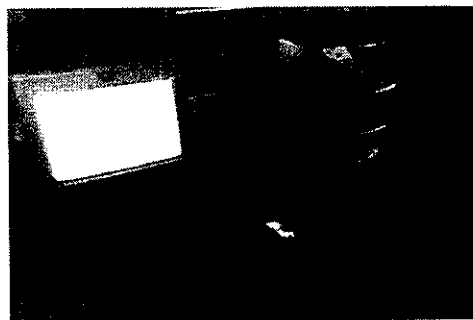


Figure 3.2 Photographic view of the setup

The Figure 3.1 shows the experimental setup used for the project. The 3 ϕ supply is given to the induction motor Figure 3.2 (a). From the terminals of the motor, connections are taken from any phase terminal (here phase B) and is connected to a current transformer (Figure 3.2 (b)), which steps down the stator current value. As the computer accepts any signal in the form of voltage, so a rheostat (Figure 3.2 (b)), is connected to convert the current to voltage. To set that voltage level to 1v, a CRO is connected across the rheostat to set the range. Across the CRO (Figure 3.2 (b)), a stereo cable (shown in dotted lines in Figure 3.1), is connected to the microphone input of the computer.

The Real Time Analyzer accepts the voltage in the form of sinusoidal waveform and does the FFT analysis and shows the spectrum of the stator current. If any broken sections in the rotor bar or end-ring, it shows the presence of harmonics at the specified frequency in the form of spikes. And to determine the number of broken rotor bars or the number of sections in the end ring, the fuzzy logic approach is used.

3.1.2 Component Specification

3.1.2.1 Induction motor specification

A three phase, 50 Hz squirrel cage induction motor is used. The rotor being casted type made of Aluminum molded bars. Totally there are 28 rotor bars and we have done the analysis for 7 broken bars. The Motor specification is,

Power	:	1HP
Rated voltage	:	415 V
Speed	:	960 rpm
Poles	:	6
No load current	:	1.7 A
No. of rotor bars	:	28

3.1.2.2 Current Transformer

Here a current transformer of step down ratio 100:5 is used. The no load line current of 1.2A is being stepped down to 50mA and it is converted in to an equivalent voltage signal by connecting a resistor in series with the secondary coil.

3.1.2.3 Rheostat

A rheostat is used to get a voltage output at its terminals. The voltage obtained will be 1v and it is transferred to the system. The device used here is a 300 Ω rheostat. The voltage is adjusted in order to bring it within the acceptable range of computer.

3.1.2.4 Stereo Cable

The input voltage is given to the PC's microphone input terminal by means of a stereo cable. Since the voltage is already stepped down to compatible level, there is no need of any ohmic connector to limit the voltage.

3.1.2.5 A/D Converter

By means of the stereo cable we are giving analog voltage signal to the sound card. There it is converted into a digital form by means of an inbuilt 16 bit A/D converter. Since the precision of the converter is well enough there is no need of any external converter.

3.1.2.6 Real Time Analyzer

Here in order to perform FFT analysis on the input current spectrum we are making use of "real time analyzer". It permits the analog waveform to be directly recorded by the PC. Further analysis can be performed by making use of the stored wave.

3.1.2.7 Fuzzy Logic

In order to interpret the results, fuzzy logic for diagnosis is used. Fuzzy logic is employed for its flexibility and easy usage. The results produced by various defuzzification methods are compared.

3.1.3 Lower Sideband and Upper Sideband Frequency

The frequency range at which the lower sideband $(1-2s)f$ and upper sideband $(1+2s)f$ are obtained as follows,

$$\begin{aligned}\text{Slip (s)} &= \frac{\text{Synchronous speed (Ns)} - \text{Rotor speed (N)}}{\text{Synchronous speed (Ns)}} \\ &= \frac{1000 - 960}{1000}\end{aligned}$$

$$\text{Slip (s)} = \mathbf{0.04}$$

$$\text{Supply Frequency (f)} = \mathbf{50 \text{ Hz}}$$

$$\begin{aligned}\text{Lower sideband Frequency} &= (1-2s) f \\ &= (1-(2*0.04))*50 \\ &= \mathbf{46 \text{ Hz}}\end{aligned}$$

$$\begin{aligned}\text{Upper sideband Frequency} &= (1+2s) f \\ &= (1+(2*0.04))*50 \\ &= \mathbf{54 \text{ Hz}}\end{aligned}$$

3.2 SOFTWARE DESCRIPTION

In online monitoring the fault is analyzed in the running condition. The stator line current is monitored by converting it into an equivalent voltage by means of a current transformer and a parallel rheostat. Then the waveform is analyzed using FFT to measure the amplitude of the side band harmonics. The block diagram is shown in the figure 3.1.

3.2.1 Real Time Analyzer

The stator current spectrum is converted into an equivalent voltage and recorded in the PC by means of a stereo cable through the microphone input terminal. The input voltage level to the PC sound card is adjusted by means of a potential divider to the acceptable level

of the sound card. It is normally 1V (peak to peak). The waveforms are recorded for various numbers of broken bars. In order to perform FFT analysis on the input waveform a “real time analyzer” (figure 3.3) is used. It permits the analog waveform to be directly recorded by the PC. It is a part of “Acoustic Analyzing System” which mainly analyzes sound waveforms. The main advantage of using this analyzer is that it permits the analog waveform to be recorded directly and it is digitized by means of inbuilt A/D converter of the PC’s sound card.

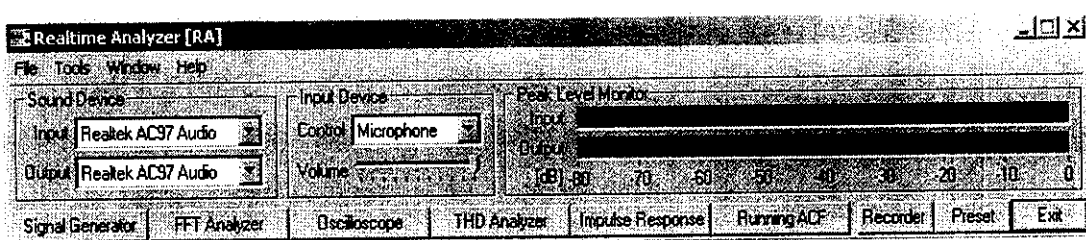


Figure 3.3 Real time analyzer

The following description specifies about the main parts of the analyzer and its function. The three main functions that are used for this project are Recorder, Oscilloscope, and FFT Analyzer.

3.2.1.1 Oscilloscope

The Real-time Analyzer is equipped with a Peak Level Monitor. If an oscilloscope is connected to the output terminal of the sound system under tests, problems in transition phenomena related to line connections, earths, and levels will be visible on the oscilloscope screen. Any momentary variances from normal test signals can be investigated immediately.

If the oscilloscope (figure 3.4) is used in combination with the signal generator, it becomes possible to easily check for distortions caused by errors in dynamic ranges for A/D-D/A converters or various types of built-in PC analog amps. From the results of these checks, the user can adjust the software volume on the software mixer, or the program volume on the A/D-D/A converters. Confirmation of the accuracy of these signals is a fundamental rule of measurement.

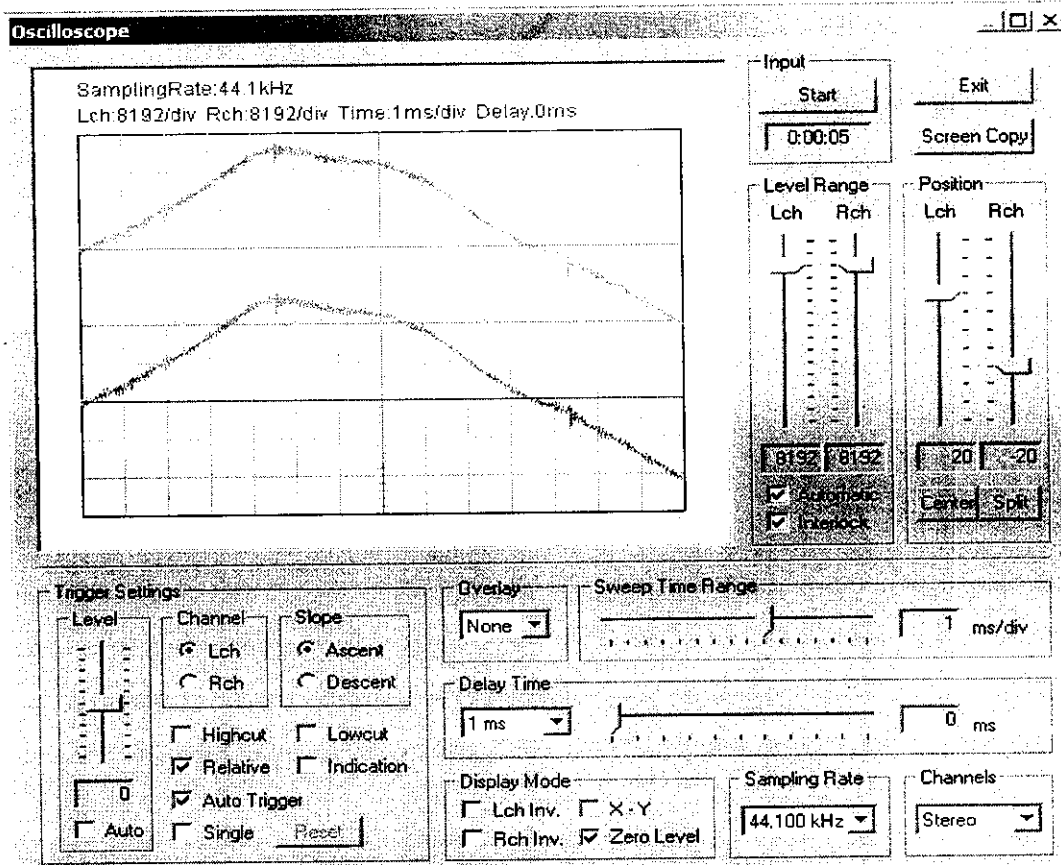


Figure 3.4 Oscilloscope

The real-time analyzer software can measure not only sound but also voltage in small electronic circuits. Actually, the soundcard can input any electric signal, though the attenuator is needed if the signal voltage exceeds the maximum voltage of the soundcard. Here a rheostat is used to step down the voltage level.

3.2.1.2 Recorder

The stereo cable carries the voltage across the rheostat to the computer. The amplitude waveform is recorded and saved in this analyzer. During the online monitoring period the recorder mode is selected to record the waveform and that can be recorded for sufficient time (sec). The figure 3.5 shows the Recorder option, during the playback mode.

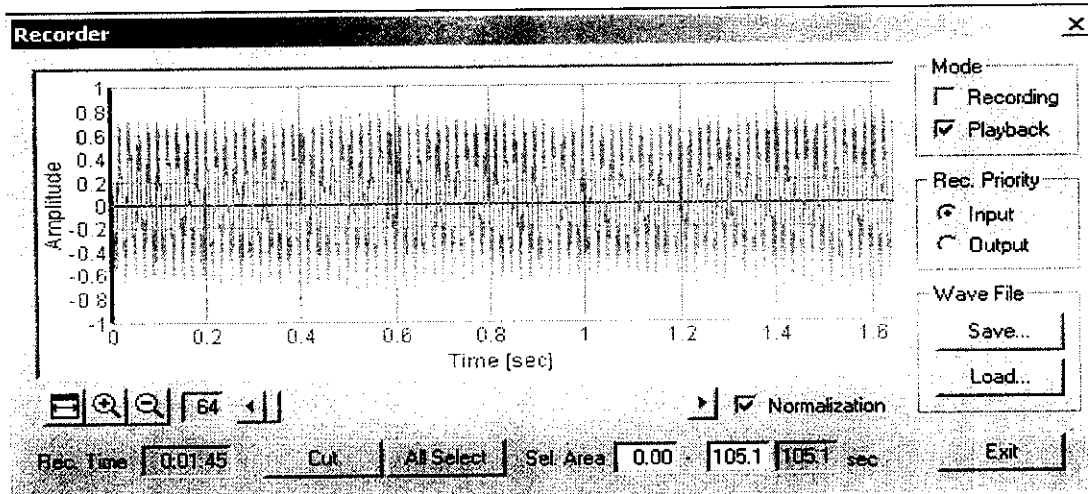


Figure 3.5 Recorder

Here the waveform shows the amplitude level of the induction machine with four broken rotor bars. The motor is made to run for about 105 sec and the corresponding waveform is recorded.

3.2.1.3 FFT analyzer

By means of FFT analyzer we can perform Fast Fourier Transform on the recorded waveform. The amplitudes of various frequency components are displayed. The displayed data can also be recorded every second. We can see the displayed waveform in the form of octave band, waterfall, correlation, spectrogram, power spectrum and phase. Calibration can also be performed in this FFT analyzer.

This gives a clear indication of the amplitude level at each frequency. The mouse pointer can be used to indicate the amplitude level at required frequency i.e. at 46 and 54Hz. When using the octave band, the “data record” can be used to record the amplitude level at each frequency during the entire time (sec) period of run. “Screen copy” is used to get the view of the spectrum wave.

The figure 3.6 shows the FFT analyzer option. Various specifications of the amplitude wave can be adjusted, like sampling rate, FFT size, channel mode, time resolution. The frequency range and the db level range can also be adjusted as per the requirement.

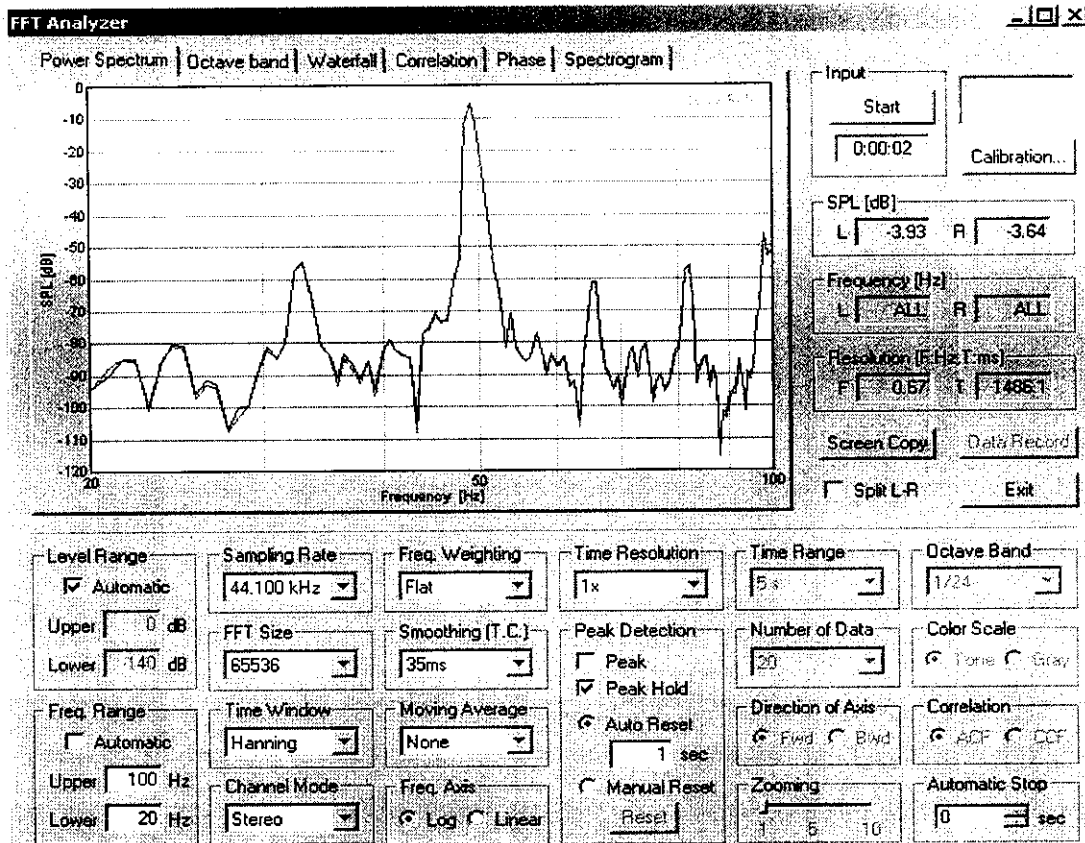


Figure 3.6 FFT Analyzer

3.3 EXPERIMENTAL RESULTS

Using this analyzer the on-line monitoring of the induction motor is done. The motor is made to run and the stator current is recorded using this analyzer. The recording is also done for various broken conditions in the rotor and the end ring. First the amplitude waveforms and amplitude levels for the condition of 14 Broken Rotor bar is shown below.

3.3.1 Broken Rotor Bar on No-Load condition

The healthy condition induction motor is made to run and its corresponding waveform and amplitude level is recorded. After that, the rotor is removed and holes are made in the rotor bars and the motor is brought to unsymmetrical condition. The fault

condition of the rotor bars can be seen in the figure 3.7. And then the motor is made to run and the corresponding amplitude waveforms and amplitude level is found.

The process is continued for many broken rotor bars. Thus the amplitude table is got for various broken bar conditions.

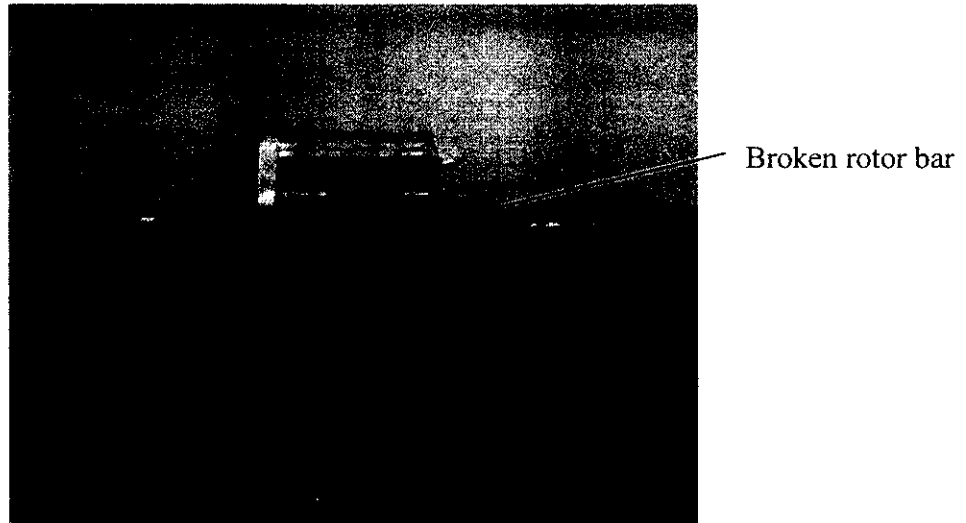


Figure 3.7 Photographic view of broken rotor

3.3.1.1 Stator Current Spectrum at various broken bar conditions

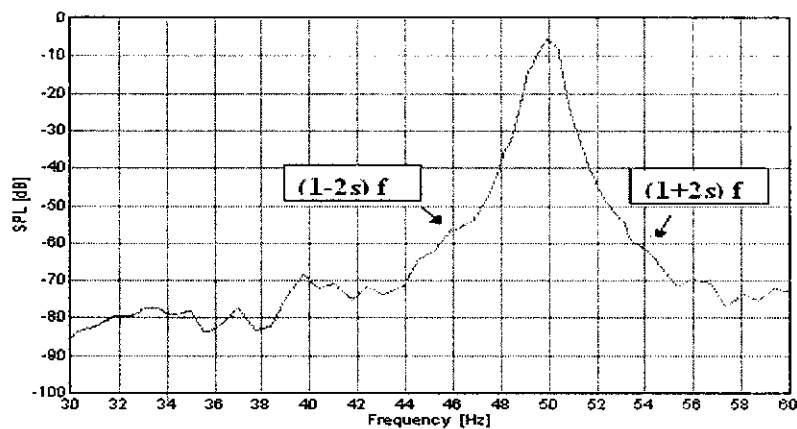


Figure 3.8 Stator Current Spectrum of a healthy motor

As said in the 2nd chapter about the rotor asymmetry due to broken rotor bar and end ring, the harmonic effect can be seen at the frequencies 46Hz and 54Hz. As in the above figure 3.8, during healthy condition there won't be any harmonics present at these frequencies.

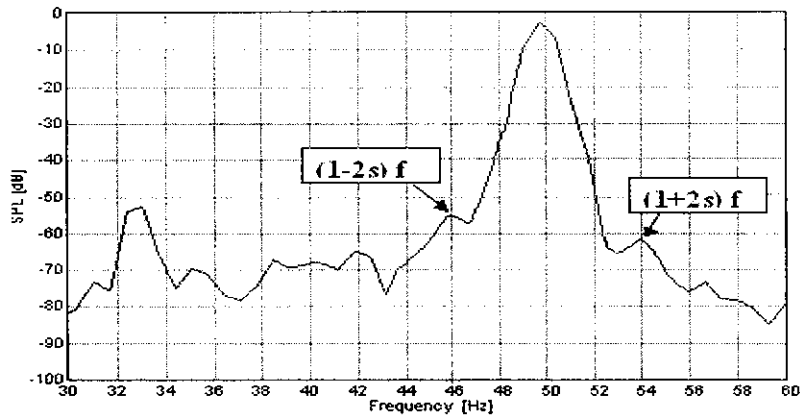


Figure 3.9 Stator current spectrum at one broken rotor bar

The figure 3.9 shows the indication of harmonics at the frequencies 46Hz and 54Hz. Due to the presence of one broken bar, the effect on its stator current can be analyzed by this figure. So due to the harmonics, the amplitude level will be higher when compared with the previous value. Therefore, the amplitude level will get higher and higher when there is more number of broken bars.

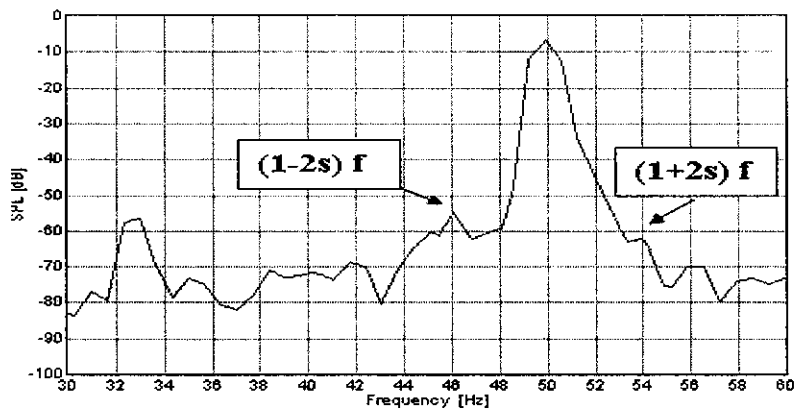


Figure 3.10 Stator current spectrum at two broken rotor bars

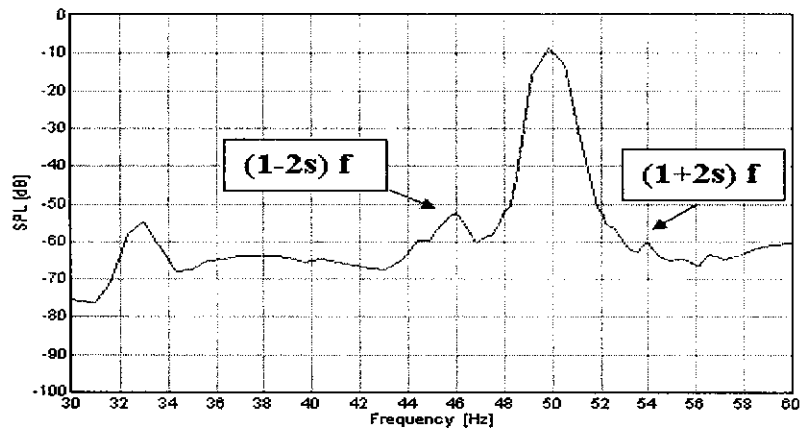


Figure 3.11 Stator current spectrum at three broken rotor bars

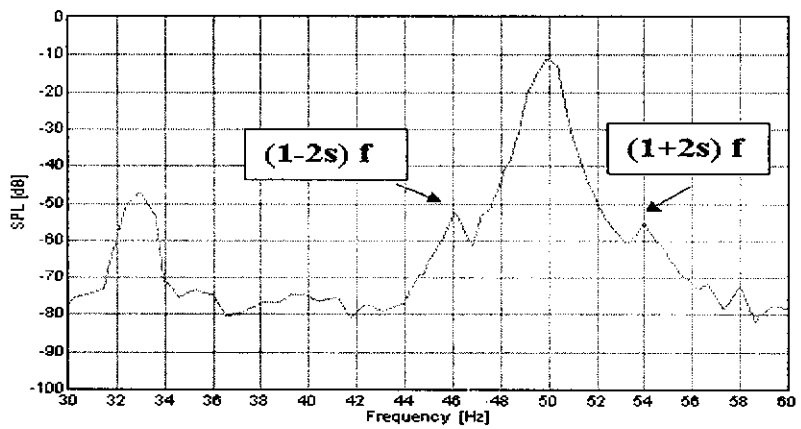


Figure 3.12 Stator current spectrum for four broken rotor bars

But it can be seen that there are harmonics present at other frequencies other than 46Hz and 54Hz. Those harmonics may occur due to other failures in the machine.

After seven broken bars, the amplitude variation won't be linear. So the fault diagnosis is done only for seven broken rotor bar conditions. The large variation in the amplitude can be seen for the amplitude table (3.1).

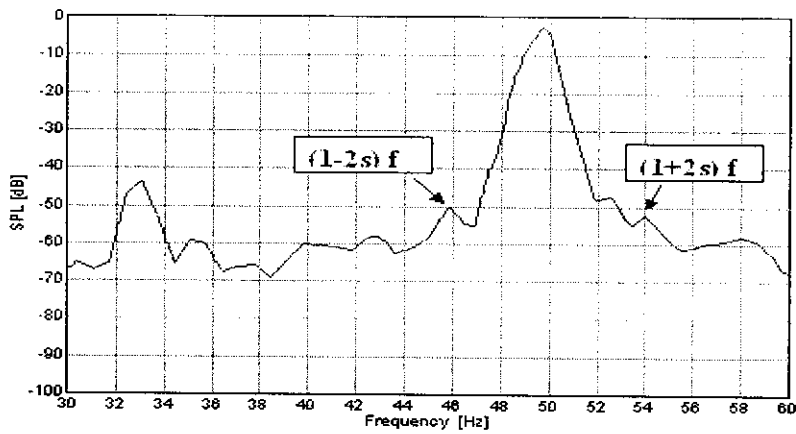


Figure 3.13 Stator current spectrum at five broken rotor bars

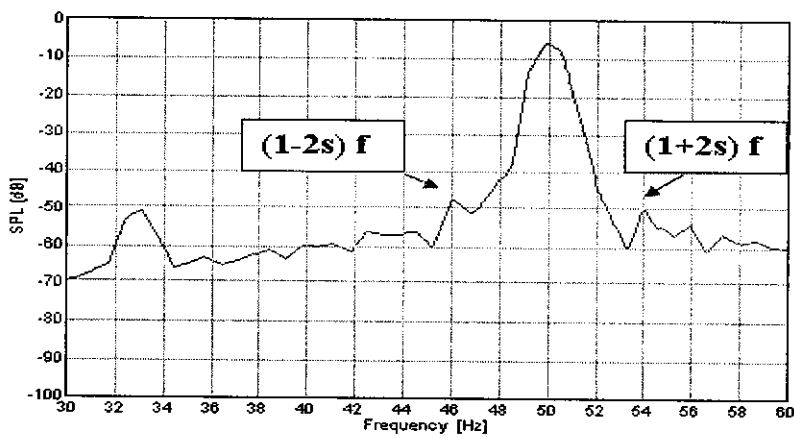


Figure 3.14 Stator current spectrum for six broken rotor bars

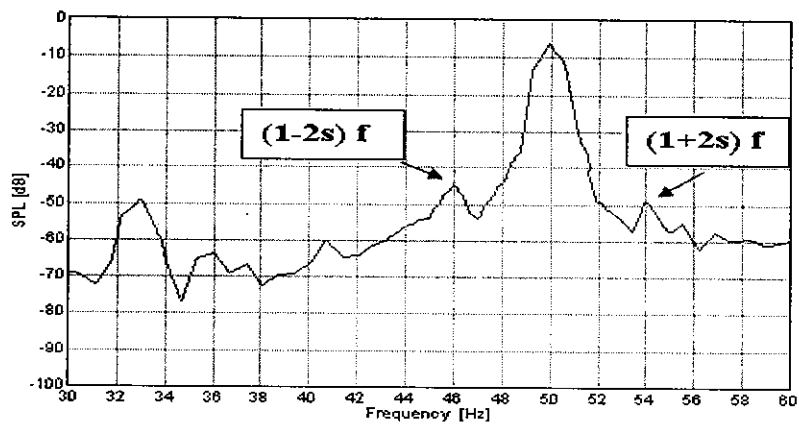


Figure 3.15 Stator current spectrum for seven broken rotor bars

3.3.1.2 Harmonic Amplitudes

The output of the FFT analyzer will be an amplitude Vs frequency graph in spectrum wave as shown in the Figures. For analysis, the two side band components of frequency $(1-2s)f$ and $(1+2s)f$ are considered and the values are denoted as amplitudes A_1 and A_2 respectively and tabulated. With this the amplitudes at the 50Hz frequency is also noted for all the cases of broken bars. The amplitudes of the side bands are noted in dB at a corresponding level where the amplitude is the highest at the 50Hz frequency under various broken bar conditions.

It can be seen that the amplitude values will be getting higher and higher, i.e. the harmonics will be increasing at the side band frequencies. As said above, after the seventh broken bar condition the amplitude values won't be gradually increasing. The values will be invariant and won't be linear.

The amplitude values of the motor on No-load condition and Load condition is shown below. On no-load condition the brake drum will be free and there won't be any spring balance attached to it. The table 3.1 and 3.2 shows the amplitudes at no-load condition and for the half load condition the brake drum is coupled with a spring balance and its amplitude values are noted.

No-Load Condition:

No. of Broken Rotor Bars	A1 (46Hz) dB	A2 (54Hz)dB
	lower sideband frequency	upper sideband frequency
0(healthy)	-56.92	-61.8
1	-55.19	-61.58
2	-54.71	-61.06
3	-54.35	-60.32
4	-51.82	-54.81
5	-50.5	-52.4
6	-48	-50
7	-45	-49

Table 3.1 Harmonic amplitudes for no-load condition of broken rotor bars

3.3.2 Broken Rotor Bar at half-Load Condition

In the load condition the brake drum of the motor is coupled with a spring balance.

3.3.2.1 Stator Current Spectrum at half-Load condition

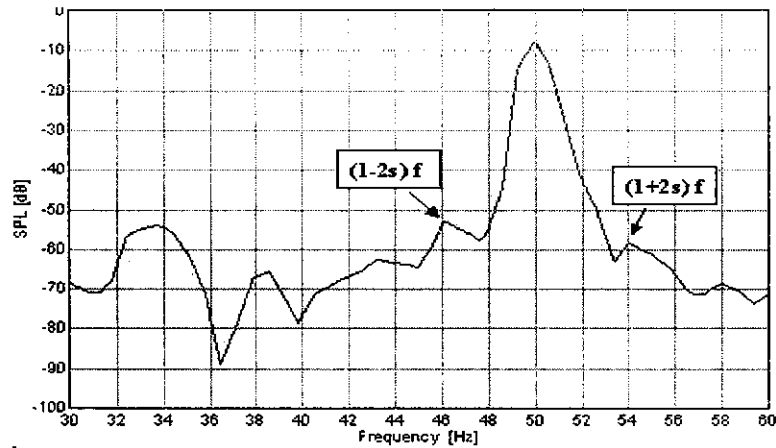


Figure 3.16 Stator currents spectrum at one broken rotor bar

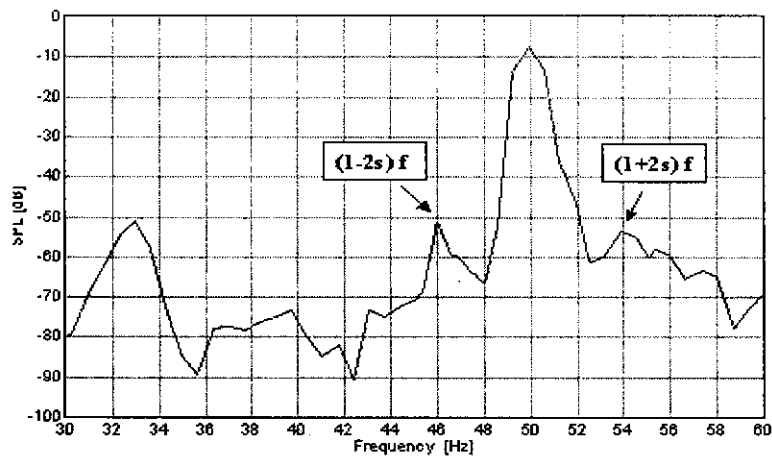


Figure 3.17 Stator current spectrum for two broken rotor bar

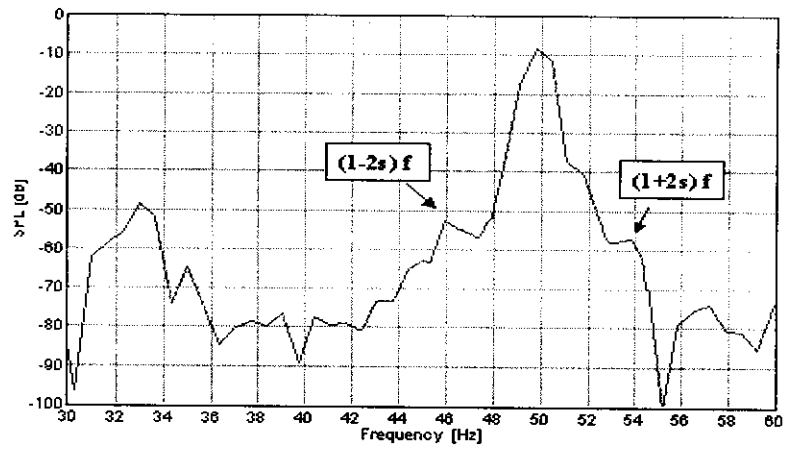


Figure 3.18 Stator current spectrum at three broken rotor bar

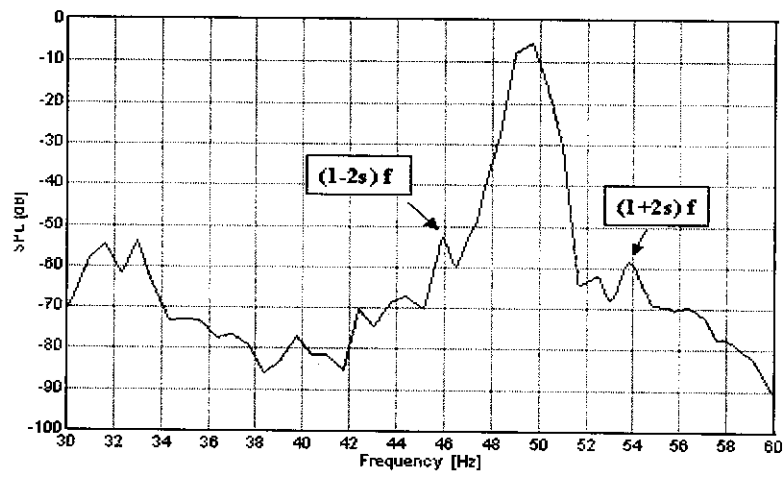


Figure 3.19 Stator current spectrum at four broken rotor bar

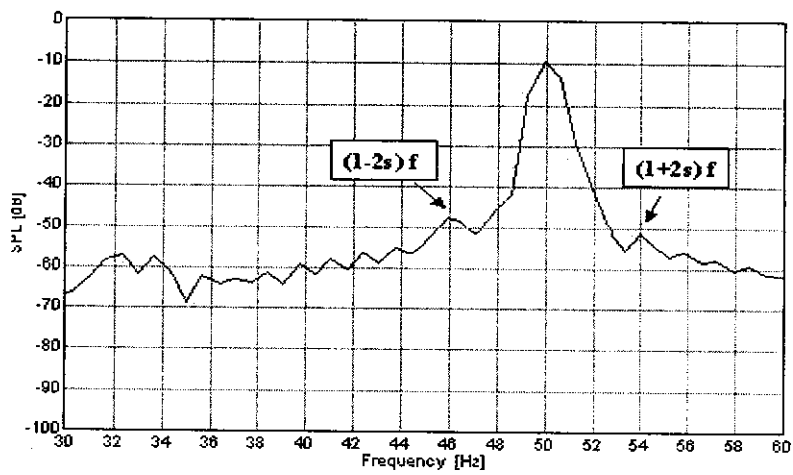


Figure 3.20 Stator current spectrum at five broken rotor bar

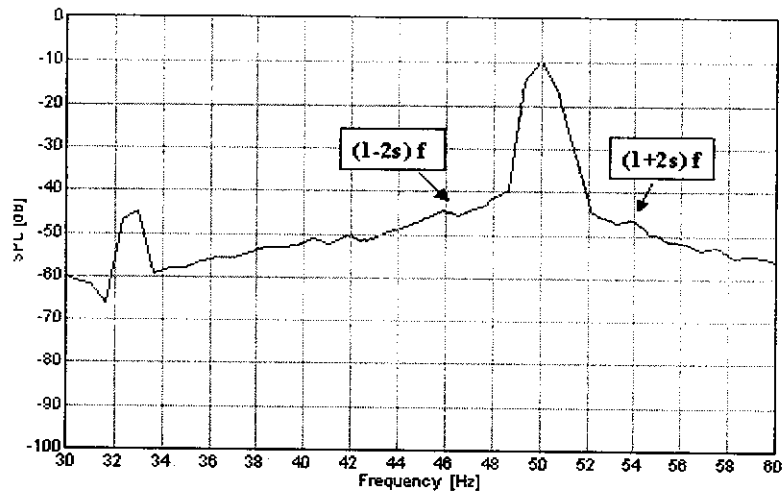


Figure 3.21 Stator current spectrum for six broken rotor bar

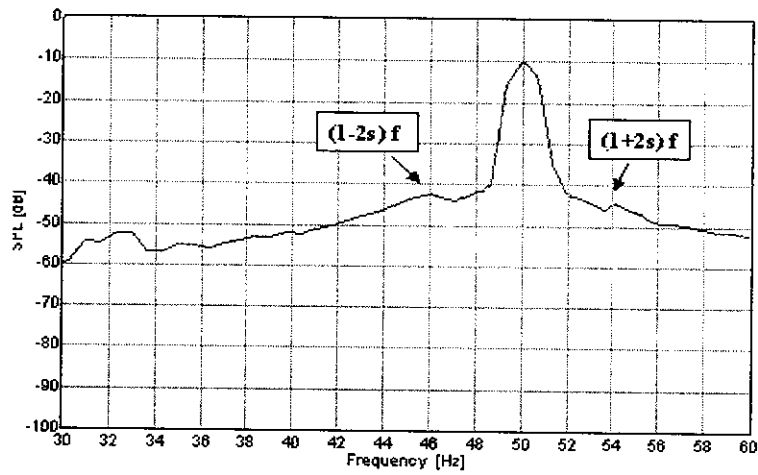


Figure 3.22 Stator current spectrum for seven broken rotor bar

3.3.2.2 Harmonic Amplitudes

No. of Broken Rotor Bars	A1 (46Hz) dB	A2 (54Hz)
	lower sideband frequency	upper sideband frequency
0(healthy)	-56.92	-61.8
1	-53.84	-59.7
2	-53.2	-58.5
3	-52	-57.8
4	-50.3	-53.6
5	-48.5	-51.92
6	-45	-47.5
7	-41.6	-45.7

Table 3.2 Harmonic amplitudes for half-load condition of broken rotor bar

3.3.3 Broken End Ring Condition

The healthy condition induction motor is made to run and its corresponding waveform and amplitude level is recorded. Then the rotor is removed and the end ring is cut using hacksaw blade at a section between rotor bars (fig 3.23). Then the motor is made to run and the corresponding amplitude waveforms and amplitude level is recorded.

The process is continued for many broken end ring sections. Thus the amplitude table is obtained for various broken end ring conditions.

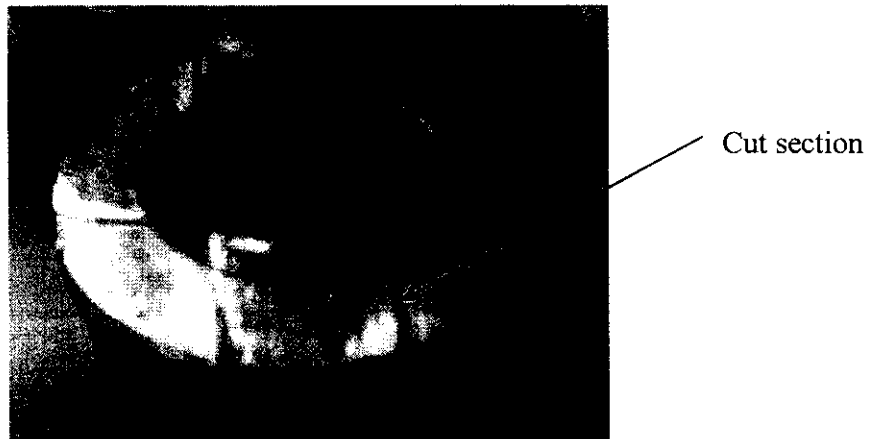


Figure 3.23 Photographic view of broken end ring

As discussed earlier, any broken (unsymmetrical) condition in the end ring may cause harmonics at only the frequency $(1-2s)f$, i.e. only the lower side band frequency will get affected. In the above figure of a broken section in end ring, the spikes are present only at 46Hz frequency. When the number of cut section increases the amplitude also get increased. It is shown in the table 3.3

3.3.3.1 Stator Current Spectrum

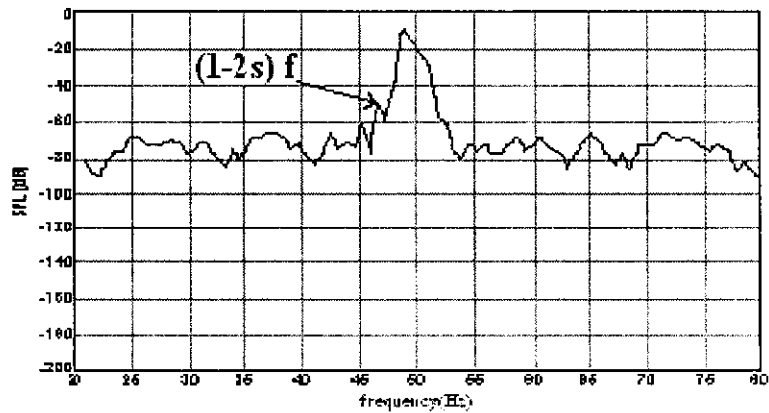


Figure 3.24 Stator current spectrum at one broken section in end ring

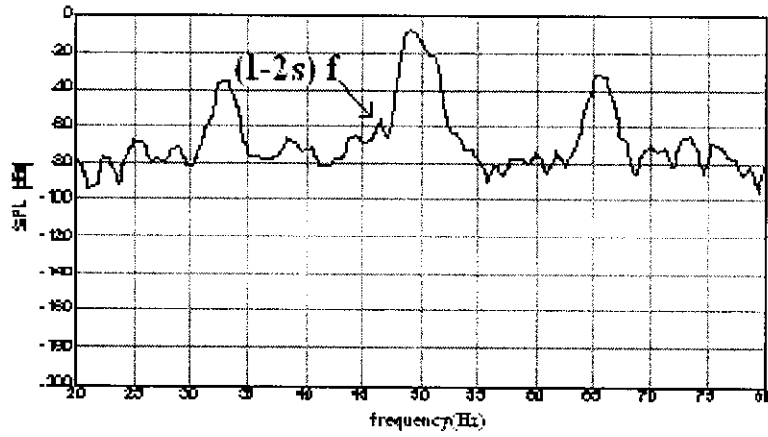


Figure 3.25 Stator current spectrum at two broken sections in end ring

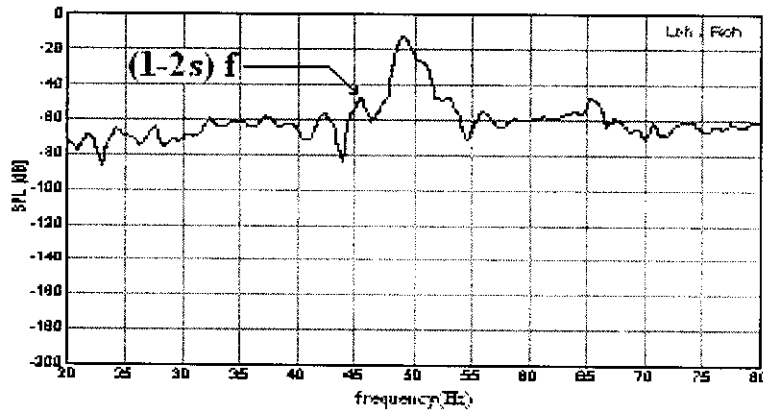


Figure 3.26 Stator current spectrum at three broken sections of end ring

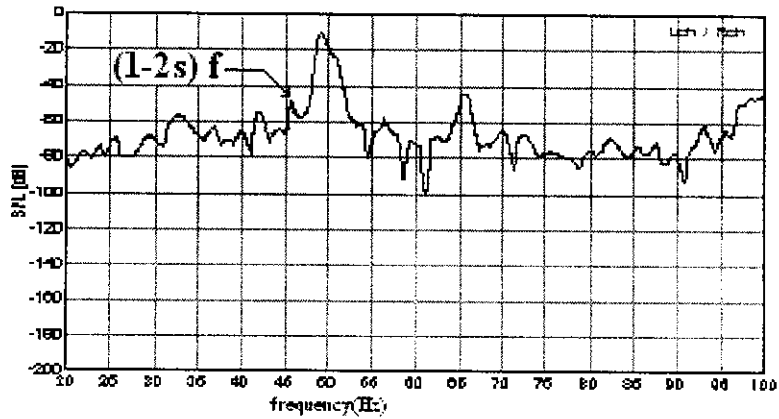


Figure 3.27 Stator current spectrum at four broken sections of end ring

3.3.3.2 Harmonic Amplitudes

No. of Broken End Ring Sections	A1 (46Hz) dB Lower sideband frequency
0(healthy)	-56.92
1	-54.56
2	-54.03
3	-49.99
4	-45.6
5	-39.19

Table 3.3 Harmonic amplitudes for broken end ring

CHAPTER-4
FUZZY LOGIC BASED FAULT DIAGNOSIS

CHAPTER-4

FUZZY LOGIC BASED FAULT DIAGNOSIS

4.1 INTRODUCTION

Fuzzy logic has two different meanings. In a narrow sense, fuzzy logic is a logical system, which is an extension of multivalve logic. But in a wider sense, which is in predominant use today, fuzzy logic (FL) is almost synonymous with the theory of fuzzy sets, a theory which relates to classes of objects with unsharp boundaries in which membership is a matter of degree. In this perspective, fuzzy logic in its narrow sense is a branch of FL. What is important to recognize is that, even in its narrow sense, the agenda of fuzzy logic is very different both in spirit and substance from the agendas of traditional multivalued logical systems.

Problems in the real world quite often turn out to be complex owing to an element of uncertainty either in the parameters which define the problem or in the situations in which the problem occurs.

The uncertainty may arise due to partial information about the problem, or due to information which is not fully reliable, or due to inherent imprecision in the language with which the problem is defined, or due to receipt of information from more than one source about the problem which is conflicting. It is in such situations that fuzzy set theory exhibits immense potential for effective solving of the uncertainty in the problem. Fuzziness means 'vagueness'. Fuzzy set theory is an excellent mathematical tool to handle the uncertainty arising due to vagueness.

Fuzzy logic systems are universal function approximates. In general, the goal of the fuzzy logic system is to yield a set of outputs for given inputs in a non-linear system, without using any mathematical model, but by using linguistic rules. It has many advantages. They are

- Fuzzy logic is conceptually easy to understand. The mathematical concepts behind fuzzy reasoning are very simple. What makes fuzzy better is the "Naturalness" of its approach and not its far-reaching complexity.
- Fuzzy logic is flexible. Fuzzy logic is tolerant of imprecise data. Everything is imprecise if you look closely enough, but more than that, most things are imprecise

even on careful inspection. Fuzzy reasoning builds this understanding into the process rather than tacking it onto the end.

- Fuzzy logic can model nonlinear functions of arbitrary complexity. You can create a fuzzy system to match any set of input-output data. This process is made particularly easy by adaptive techniques like Adaptive Neuro-Fuzzy Inference Systems (ANFIS), which are available in the Fuzzy Logic Toolbox.
- Fuzzy logic can be built on top of the experience of experts. In direct contrast to neural networks, which take training data and generate opaque, impenetrable models, fuzzy logic lets you rely on the experience of people who already understand your system.

Fuzzy logic is based on natural language. The basis for fuzzy logic is the basis for human communication. This observation underpins many of the other statements about fuzzy logic.

4.2 MAMDANI FUZZY INFERENCE SYSTEM:

Mamdani-type of fuzzy logic controller contains four main parts (fig 4.1), two of which perform transformations. The four parts are

- Fuzzifier (transformation 1)
- Knowledge base
- Inference engine(fuzzy reasoning, decision-making logic)
- Defuzzifier(transformation 2)

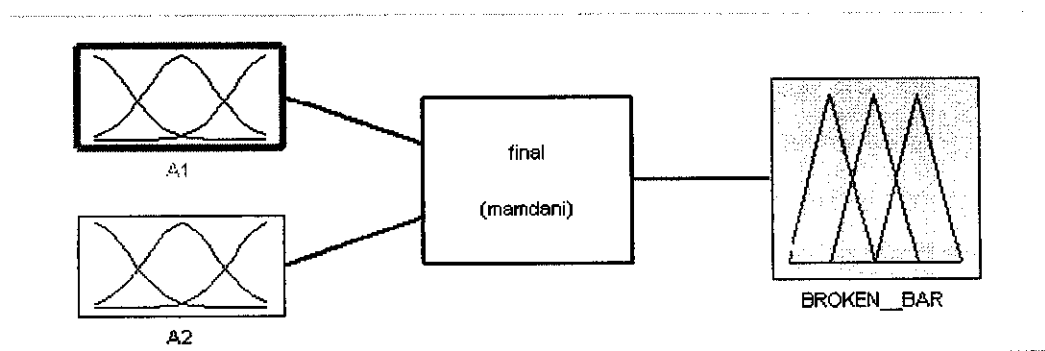


Figure 4.1 Mamdani fuzzy inference System

4.2.1 Fuzzifier

The fuzzifier performs measurement of the input variables (input signals, real variables), scale mapping and fuzzification (transformation 1). Thus all the monitoring input signals are scaled and fuzzification means that the measured signals (crisp input quantities which have numerical values) are transformed into fuzzy quantities. This transformation is performed by using membership functions. In a conventional fuzzy logic controller, the number of membership functions and the shapes of these are initially determined by the user.

4.2.2 Knowledge Base

The knowledge base consists of the data base and the linguistic control rule base. The data base provides the information which is used to define the linguistic control rules and the fuzzy data manipulation in the fuzzy logic controller. The rule base specifies the control goal actions by means of a set of linguistic control rules. In other words, the rule base contains rules such as would be provided by an expert. The fuzzy logic controller looks at the input signals and by using the expert rules determines the appropriate output signals (control actions). The rule base contains a set of if-then rules.

4.2.3 Inference Engine

It is the kernel of a fuzzy logic controller and has the capability both of simulating human decision-making based on fuzzy concepts and of inferring fuzzy control actions by using fuzzy implication and fuzzy logic rules of inference. In other words, once all the monitored input variables are transformed into their respective linguistic variables, the inference engine evaluates the set of if-then rules and thus result is obtained which is again a linguistic value for the linguistic variable. This linguistic result has to be then transformed into a crisp output value of the fuzzy logic control.

4.2.4 Defuzzifier

The second transformation is performed by the defuzzifier which performs scale mapping as well as defuzzification. The defuzzifier yields a non-fuzzy, crisp control action from the inferred fuzzy control action by using the consequent membership functions of the rules. There are many defuzzification techniques. They are centre of gravity method, height method, centroid method, mean of maxima method, first of maxima method, sum of maxima. In this project centroid method defuzzification technique is used.

4.2.5 Operation of fuzzy system

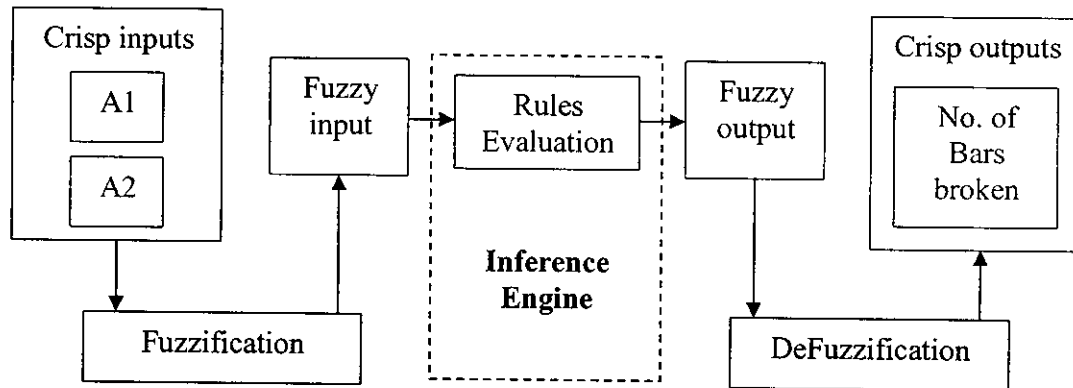


Figure 4.2 Fuzzy system

There are two numbers of crisp inputs used in this project, A1 and A2 (fig 4.2), which specifies about the two harmonic amplitudes at the frequency 46Hz and 54Hz. This is in case of broken rotor bar condition. But in the case of Broken end ring condition, there will be only one crisp input. The crisp output in the broken rotor bar condition will display the total number of broken bars and in the broken end ring condition the crisp output will display the total number of sections broken.

The inference engine does the fuzzification by using fuzzy concepts. So the crisp inputs have to be converted into fuzzy input. This process is called Fuzzification. Fuzzification converts the numerical data (crisp input) into membership functions (fuzzy input). And also the crisp output displays in the form of numerical data. So the fuzzy output (membership function) from the inference engine is converted into crisp output (numerical data). This process is called DeFuzzification.

The simulation process is done based on the fuzzy implication and fuzzy rules. The rules are framed based on the number of membership functions used in both the input and output. There will be two set of rules, one for broken rotor bar condition and other for broken end ring condition. The inference engine simulates based on the rules and displays the output for number of broken rotor bars and number of broken sections in the end ring.

4.3 FAULT DIAGNOSIS FOR BROKEN ROTOR BAR

The fuzzy logic approach is implemented to determine the number of rotor bars broken. Two inputs A1 and A2 are used and the rules are framed based on their combination to give the output. In each input functions, five membership functions are implemented. So the rules framed are;

4.3.1 Rules

- If A1 is very low and A2 is very low then No rotor bar broken.(healthy condition)
- If A1 is low and A2 is low then one broken rotor bar broken.
- If A1 is low and A2 is medium then two broken rotor bar.
- If A1 is medium and A2 is low then two broken rotor bar.
- If A1 is medium and A2 is medium then three broken rotor bar.
- If A1 is medium and A2 is high then four broken rotor bars.
- If A1 is high and A2 is medium then four broken rotor bars.
- If A1 is high and A2 is high then five broken rotor bars.
- If A1 is high and A2 is very high then six broken rotor bars.
- If A1 is very high and A2 is high then six broken rotor bars.
- If A1 is very high and A2 is very high then seven broken rotor bars.

4.3.2 Fuzzification

As shown in the rules, there will be five membership functions. The width of these five functions will be based on the value of the harmonic amplitudes.

For A1, the simulated data suggest, “very low” from -56.6 to -55.36, “low” from amplitude -55.6 to 54.4, “medium” from amplitude -54.6 to -50.3, “high” from amplitude -51.3 to 45.1 and “very high” from amplitude -45.83 to -40.8. For A2, the simulated data suggest, “very low” from amplitude -62.8 to -61.37, “low” from amplitude -61.7 to 61.16, “medium” from amplitude -61.29 to 55, “high” from amplitude -55.44 to 50 and “very high” from amplitude -51 to 47.7. For output the simulated data suggest, “0” from -0.196 to 0.479, “1” from 0.479 to 1.49, “2” from 1.34 to 2.7, “3” from 2.44 to 3.55, “4” from 3.33 to 4.74, “5” from 4.65 to 5.86, “6” from 5.57 to 6.47, “7” from 6.37 to 7.62. The amplitude of the fault components increases with the number of broken rotor bars.

As the same rules are used for the broken rotor bar detection in load condition, same numbers of membership functions are used for the fuzzy logic approach. The membership functions used are shown in the figures (4.3, 4.4 and 4.5);

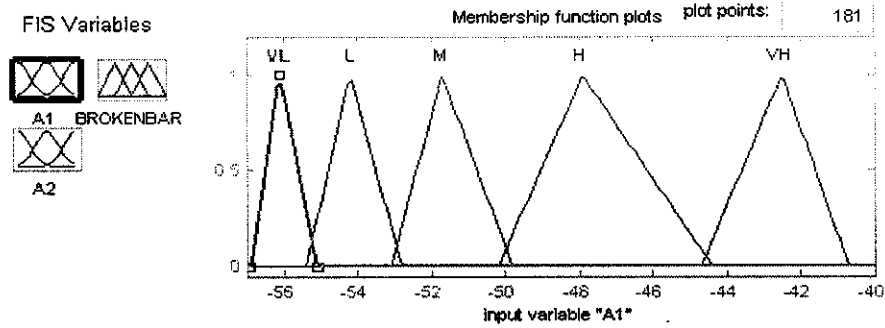


Figure 4.3 Membership function for A1

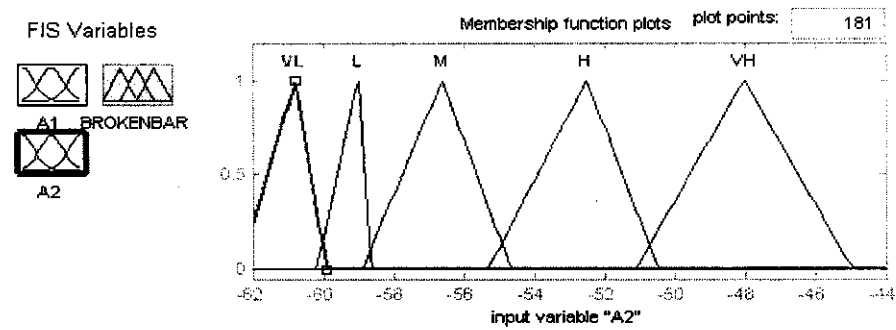


Figure 4.4 Membership function for A2

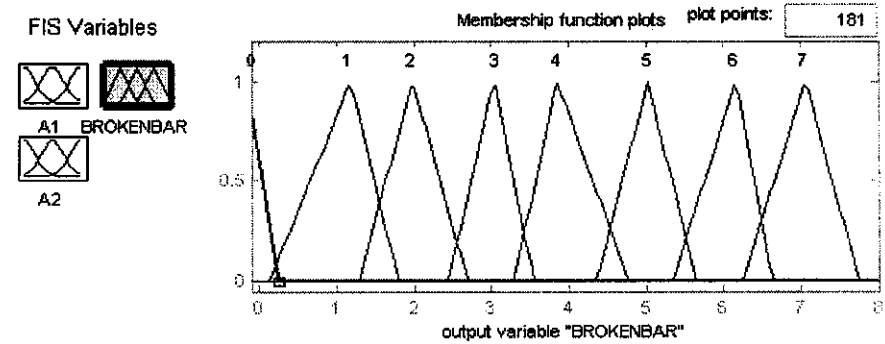


Figure 4.5 Membership function for output

4.3.3 Simulation Result

The fuzzy approach is performed and the output is obtained to determine the number of broken rotor bars in no-load condition and load condition. The actual value and the observed value are compared and the percentage of error is calculated. This is calculated to check the performance and its efficiency.

The error is calculated by the formula,

$$\frac{| \text{Actual value} - \text{observed value} |}{\text{Actual value}} * 100$$

The results obtained are shown in the table 4.1 and 4.2, at no-load condition...

Input (A1) 46 Hz dB	Input (A2) 54 Hz dB	o/p Actual value	o/p Observed value	%error
-56.92	-61.8	0	0.004	0
-55.19	-61.58	1	1.01	1
-54.71	-61.06	2	2.02	1
-54.35	-60.32	3	3.01	0.33
-51.82	-54.81	4	4.02	0.5
-50.5	-52.4	5	5	0
-48	-50	6	6.01	0.16
-45	-49	7	7	0

Table 4.1 Simulation result of broken rotor bar in no-load condition

In half-load condition...

Input (A1) 46 Hz dB	Input (A2) 54 Hz dB	o/p Actual value	o/p Observed value	%error
-56.92	-61.8	0(healthy)	0.002	0
-53.84	-59.7	1	1	0
-53.2	-58.5	2	2	0
-52	-57.8	3	3	0
-50.3	-53.6	4	4.01	0.25
-48.5	-51.92	5	5.01	0.2
-45	-47.5	6	6	0
-41.6	-45.7	7	7	0

Table 4.2 Simulation result of broken rotor bar in load condition

4.4 FAULT DIAGNOSIS FOR BROKEN END RING

The fuzzy logic approach is done to determine the number of sections broken at the end ring. As explained in the effects of broken end ring, the lower side band frequency is disturbed with the harmonics. So the spikes will be present only in the frequency of 46Hz. One input A1 is used as the amplitude and based on the level of that amplitude the number of sections broken at the end ring is calculated. Five membership functions are used in the input to determine the amplitude levels.

In the end ring, as said in the experimental setup five sections are broken and so five membership functions are used. So the rules specified will be simple to determine the broken end ring sections.

4.4.1 Rules

- If input is very low then one end ring section broken.
- If input is low then two end ring sections broken.
- If input is medium then three end ring sections broken
- If input is high then four end ring sections broken.
- If input is very high then five end ring sections broken.

4.4.2 Fuzzification

As shown in the rules there will be five membership functions to determine the number of sections broken in the end ring. The width of these five membership functions is based on the amplitude levels.

As shown in the figures 4.6 and 4.7, For A1 the simulated data suggest, “very low” from -63.8 to -54.01, “low” from -54.4 to -51.7, “medium” from -52 to -47.02, “high” from -47.7 to -40.4 and “very high” from -40.96 to -35.36. The simulated output data suggest, “1” from 0.46 to 1.53, “2” from 1.34 to 2.67, “3” from 2.37 to 3.59, “4” from 3.31 to 4.69 and “5” from 4.5 to 5.55.

The membership functions are shown below;

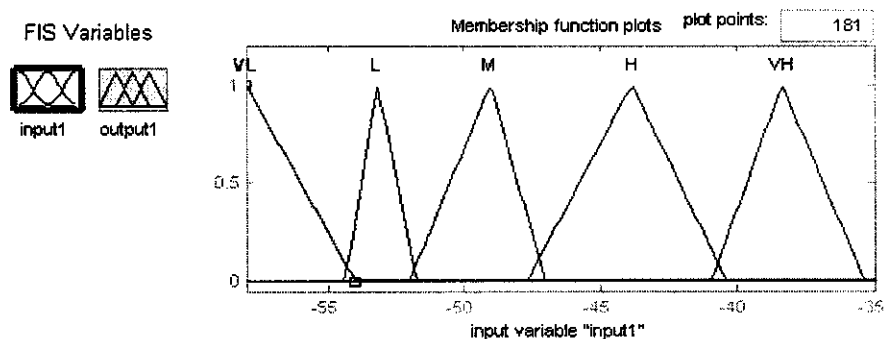


Figure 4.6 Membership function of input A1

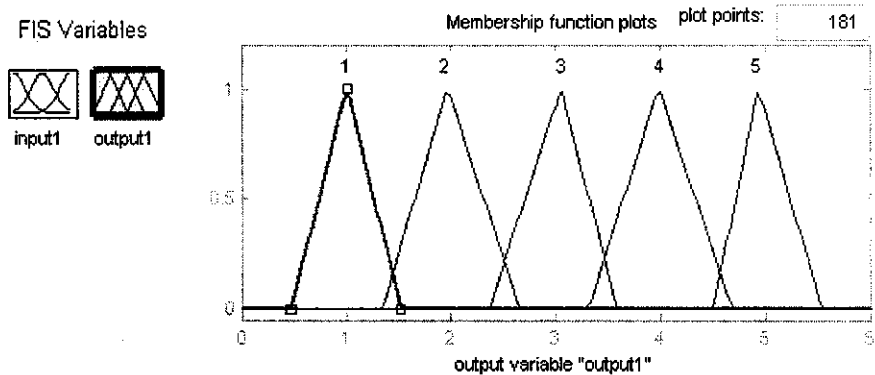


Figure 4.7 Membership function of the output

4.4.3 Simulation Result

The fuzzy logic approach is done to determine the number of sections broken in the end ring. The actual value and the observed values are compared and the percentage of error is calculated to find the performance and efficiency of the approach (table 4.3).

The error is calculated using the same formula used for the broken rotor bar detection.

Input (A1) 46 Hz dB	Output Actual value	Output Observed value	%error
-54.56	1	0.999	0.1
-54.03	2	1.99	1.5
-49.99	3	3	0
-45.6	4	4	0
-39.19	5	5	0

Table 4.3 Simulation result for broken end ring

4.5 SOFTWARE DESIGN

A similar software approach is done to find the status of both the end ring and rotor bars by checking their amplitudes at the specified frequencies. Software is specially designed for the purpose. First the stator current pattern is recorded from the pc sound card. The required FFT analysis is performed by the programming code in the software. The required current spectrum is obtained from the FFT analysis at the specified frequency. At this specified frequency (46 Hz and 54 Hz) the amplitude level is obtained and displayed. Then the side band amplitude is fuzzified by the program code. The result such as the status of broken rotor bar and end ring and the side band amplitude levels are displayed along with its current spectrum. The main advantage of this Software is, Effective On-line Monitoring is possible.

4.5.1 Algorithm

- Step 1: Start.
- Step 2: To record current signal from the sound card.
- Step 3: Perform FFT analysis.
- Step 4: Extract amplitude at the particular frequency.
- Step 5: Perform fuzzy diagnosis.
- Step 6: Display the status of End ring and Rotor bar.

4.5.2 Flowchart

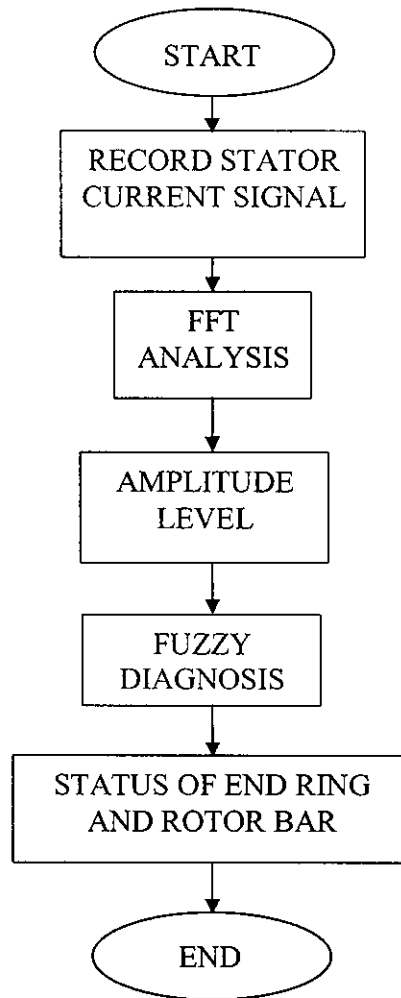


Figure 4.8 Flowchart of Software algorithms

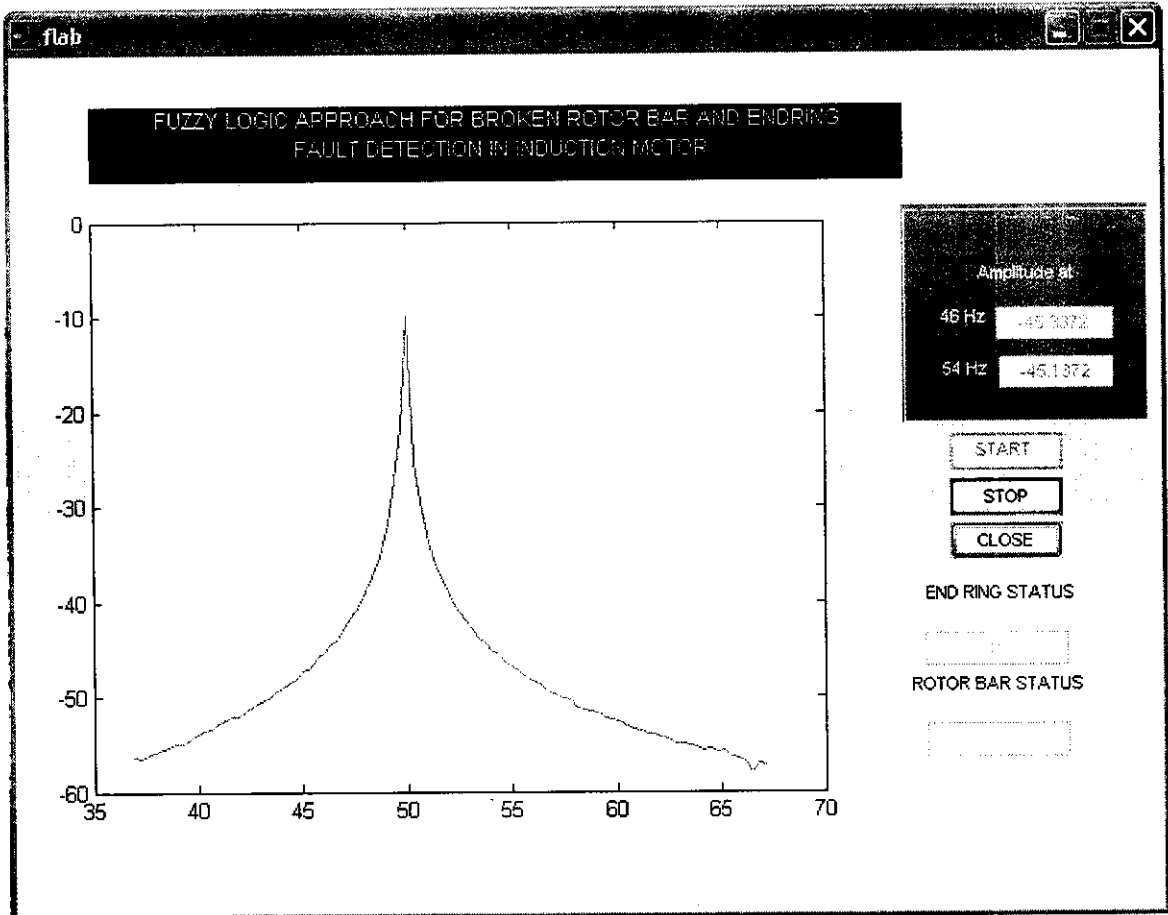


Figure 4.9 Picture of the Software

CHAPTER-5
CONCLUSION

CHAPTER-5

CONCLUSION

5.1 CONCLUSION OF THE PROJECT

An On-Line broken rotor bar and end ring fault detection scheme has been developed for three phase squirrel cage induction motor. The Fuzzy Logic has been used to diagnose the faults. The status of the rotor bar and End Ring is monitored.

5.2 FUTURE SCOPE

- The bearing condition can also be analyzed for fault diagnosis.
- The fault detection scheme can be carried out using Neuro-fuzzy techniques.
- Rules can be optimized using genetic algorithm.

Program

```
function varargout = flab(varargin)
    gui_Singleton = 1;
    gui_State = struct('gui_Name',    mfilename, ...
        'gui_Singleton', gui_Singleton, ...
        'gui_OpeningFcn', @flab_OpeningFcn, ...
        'gui_OutputFcn', @flab_OutputFcn, ...
        'gui_LayoutFcn', [] , ...
        'gui_Callback', []);
    if nargin && ischar(varargin{1})
        gui_State.gui_Callback = str2func(varargin{1});
    end

    if nargout
        [varargout{1:nargout}] = gui_mainfcn(gui_State, varargin{:});
    else
        gui_mainfcn(gui_State, varargin{:});
    end

function flab_OpeningFcn(hObject, eventdata, handles, varargin)
    handles.output = hObject;
    guidata(hObject, handles);
    global FLAG;
    FLAG=1;
    set(handles.stopf,'Enable','off');

function varargout = flab_OutputFcn(hObject, eventdata, handles)
    varargout{1} = handles.output;
```

```

function startf_Callback(hObject, eventdata, handles)

    set(handles.startf,'Enable','off');
    set(handles.stopf,'Enable','on');
    global FLAG;
    if(FLAG==0)
        FLAG=1;
    end
    pause(0.01);
    while FLAG==1
        eval('flab("xyz_Callback",gcbo,[],guidata(gcbo))');
        pause(0.01);
    end

```

```

function stopf_Callback(hObject, eventdata, handles)
    global FLAG;
    set(handles.startf,'Enable','on');
    set(handles.stopf,'Enable','off');
    FLAG=0;

```

```

function closef_Callback(hObject, eventdata, handles)
    close

```

```

function forty_Callback(hObject, eventdata, handles)

```

```

function forty_CreateFcn(hObject, eventdata, handles)

```

```

    if ispc

```

```

        set(hObject,'BackgroundColor','white');

```

```

    else

```

```

        set(hObject,'BackgroundColor',get(0,'defaultUicontrolBackgroundColor'));

```



```
end
```

```
function fifty_Callback(hObject, eventdata, handles)
```

```
function fifty_CreateFcn(hObject, eventdata, handles)
```

```
if ispc
```

```
    set(hObject,'BackgroundColor','white');
```

```
else
```

```
    set(hObject,'BackgroundColor',get(0,'defaultUicontrolBackgroundColor'));
```

```
end
```

```
function eresult_Callback(hObject, eventdata, handles)
```

```
function eresult_CreateFcn(hObject, eventdata, handles)
```

```
if ispc
```

```
    set(hObject,'BackgroundColor','white');
```

```
else
```

```
    set(hObject,'BackgroundColor',get(0,'defaultUicontrolBackgroundColor'));
```

```
end
```

```
function bresult_Callback(hObject, eventdata, handles)
```

```
function bresult_CreateFcn(hObject, eventdata, handles)
```

```
if ispc
```

```
    set(hObject,'BackgroundColor','white');
```

```
else
```

```
    set(hObject,'BackgroundColor',get(0,'defaultUicontrolBackgroundColor'));
```

```
end
```

```
function xyz_Callback(hObject, eventdata, handles)
```

```
    Fs = 96000;
```

```
    y = wavrecord(3*Fs,Fs,'double');
```

```
    % y = wavread('xyz.wav');
```

```
    % y = y(:,1);
```

```

size=131072*2;
Y = fft(y,size);
Pyy = abs(Y)/size;
Plog = 20 * log10(Pyy);
f = Fs*(1:size)/size;
% -- MAGNITUDE AT 46 Hz -- %
x = (f-46)/46;
for i=1:size
    if( x(i) <0)
        x(i)=x(i)*(-1);
    end
end
[c,l]=min(x);
abc = Plog(l);
% -- MAGNITUDE AT 54 Hz -- %
z = (f-54)/54;
for j=1:size
    if( z(j) <0)
        z(j)=z(j)*(-1);
    end
end
[d,m]=min(z);
def = Plog(m);
set(handles.forty,'String',abc);
set(handles.fifty,'String',def);
plot(f(10:400),Plog(10:400));
fismat1= readfis('one.fis');
out1 = evalfis(abc,fismat1);
if (out1<0.1)
    out1='0 BAR BROKEN';
else

```

```
if (out1>0.9)
    out1='4 BROKEN BAR';
else
    if(out1< 0.6 && out1>0.4)
        out1='4 BROKEN BAR';
    end
end
end
set(handles.bresult,'String',out1);
set(handles.eresult,'String','0');
```

REFERENCES

1. M.E.H Benbouzid, "Bibliography on Induction Motor Faults Detection and Diagnosis", *IEEE Transaction on Energy Conversion*, vol. 14, dec 1999.
2. F. Bangura, Nabeel A. O. Demerdash, "Diagnostics of Eccentricities and Bar/End-Ring connector Breakages in Polyphase Induction Motors through a Combination of Time series Data Mining and Time-stepping Coupled FE-state-space Techniques", *IEEE Transaction on Industry Application*, vol. 39, Aug 2003.
3. J. F. Bangura, N. A. Demerdash, "Diagnosis and Characterization of effects of Broken Bars and Connectors in Squirrel cage Induction Motor by Time stepping coupled Finite Element state space modeling approach", *IEEE Transaction on Energy Conversion*, vol. 14, dec1999.
4. Filippetti.F, Franceschini.G, Tassoni.C and Peter Vas (1994), 'Broken Bar Detection in Induction Machines: Comparison between Current Spectrum Approach and Parameter Estimation Approach', *Proceedings of the IEEE IAS Annual Meeting Conference*, Vol 1, Pp 95 -102.
5. Jafar Milimonfared, Honayoun Meshgin Kelk and Subhasis Nandi, (1999), 'A Novel Approach for Broken- Rotor – Bar Detection in Cage Induction Motor', *IEEE Transaction-Industry Application*, Vol 35, No. 5, Pp 1000 – 1005.
6. Fiorenzo Filippetti, Giovanni Franceschini, Carl Tassoni, "Recent Developments of Induction Motor Drives Fault Disgnosis Using AI Techniques", *IEEE Transaction on Industrial Electronics*, vol. 47, Oct' 2000.
7. ST. J. Manolas, J. A. Tegapoulos L, "Analysis of Squirrel cage Induction Motors with Broken bars and Rings", *IEEE Transaction on Energy Conversion*, vol. 14, Dec1999.

8. Humberto Hanao, Hubert Razik, Gerard Andre, "Analytical Approach for the Stator Current Frequency Harmonics Computation for Detection of Induction Machine Rotor Faults", *IEEE Transaction on Industrial Application*, vol. 41, May/June 2005.
9. Hamid. A. Toliyat, Thomas. A. Lipo, "Transient Analysis of Cage Induction Machines Under Stator, Rotor Bar and End Ring Faults", *IEEE Transaction on Energy Conversion*, vol. 10, June 1995.
10. H. Douglas, P. Pillay, A. K. Zairani. "Broken Rotor Bar Detection in Induction Machines with Transient Operating Speeds", *IEEE Transaction on Energy Conversion*, vol. 20, March 2005.

BIBLIOGRAPHY

1. Mo- Yeun chow, "Methodologies of Using Neural Network and Fuzzy Logic Technologies for Motor Incipient Fault Detection", *World Scientific Publishing Co. Pte. Ltd*, 1997.
2. B.L. Theraja, A.K. Theraja, "Electrical Technology Volume II", *S. Chand & Company Ltd*, 2004.